If It Walks Like an Arbitrage: Protocol-Agnostic Detection with Decidable Structural Equivalence

Adam Khayam, Hamid Kolli, Mohamed Iguernlala, Çagdas Bozman
Functori, Paris, France

arXiv:2608.20377v2 [q-fin.CP] 25 Aug 2026

***Abstract*—Whether a transaction performed an arbitrage, and by which route, is a question asked of its execution trace after the fact. We conjecture that such traces admit a normal form on which questions of this kind become queries, and we test it by building one and putting it to work. Each trace becomes an abstract syntax tree of token transfers, grouped by call-frame nesting. A term rewriting system of 16 rules reduces it. Rewriting terminates and carries exactly the transfers of the trace, whichever order the rules fire in. Under a deterministic kernel scanning the EVM-fixed trace order, every trace has a unique normal form, and the structural equivalence this induces on fund flows is decidable. Preservation, termination, soundness, uniqueness and decidability are mechanized in Rocq with zero admitted obligations. We report arbitrage detection in full: cycles emerge at the fixpoint and are read off the normal form with no protocol-specific patterns. Detection is the query we evaluate at scale; structural equivalence is a second query. The pipeline depends only on the standard ERC token and WETH ABIs, so the same binary runs unmodified on Arbitrum and BSC.**

We evaluate on two arbitrary block ranges, analysed in full with no transaction excluded: 220 000 Ethereum blocks against EigenPhi, a widely used MEV detection platform, and 1 000 shared blocks against ArbiNet, a graph neural network classifier. These are the only tools and label sets in this domain we were able to reuse. We report 469 801 confirmed arbitrages, overlapping 83.5% with EigenPhi and 81% with ArbiNet, together with 245 497 attempted arbitrages and 60 199 confirmed detections EigenPhi does not report. 99.2% follow from the fixpoint alone and are sound over the decoded transfers, and manual validation of 500 transactions finds no false positive among the confirmed. We also analyse baseline-only detections to characterize where the systems disagree.

I. Introduction

Every Ethereum transaction leaves a replayable trace of its internal calls and token movements. The record is complete, yet not self-explanatory: the same movements can be a trade, a repayment, a withdrawal, or an attack, and which one happened depends on how the execution produced the transfers, not on the transfers alone. The difference now carries legal weight. Whether a twelve-second interaction with the block-building pipeline was arbitrage or wire fraud is the substance of a federal prosecution whose first jury could not decide [1]; a fraud conviction over the Mango Markets exploit, defended as a trading strategy, was vacated on the ground that an automated contract cannot be deceived, and is on appeal [2]; and MiCA now requires venues to report manipulative transaction-ordering [3], without saying how. Surveillance, protocol design, and incident response ask the same questions of a trace after the fact: did it perform an arbitrage? Through which route? Do two transactions, under different contracts and tokens, implement the same strategy?

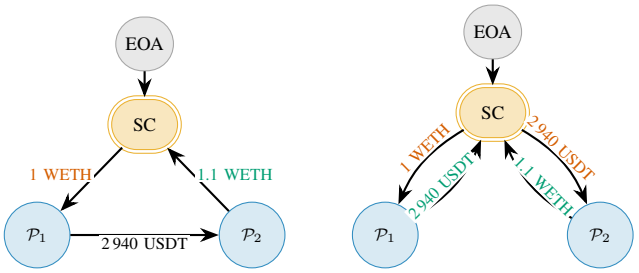

(a) Pool-to-pool flow. (b) SC-mediated flow.

Fig. 1. One arbitrage, two transfer graphs. Red: sent; green: received.

An *arbitrage*, informally, is a round trip that pays: value leaves an account in some asset and returns to it, in the same asset, in greater quantity. On Ethereum it is an industry: prices for a pair differ across automated market makers (AMM) [4], [5], [6], and bots buy where an asset is cheap and sell where it is dear, closing the loop in one atomic transaction so the trade either profits or costs only gas. This is the core of *maximal extractable value* (**MEV**), and the same mechanics, amplified by flash loans [7], [8], [9], [10], have drained millions from DeFi pools. Both conditions, returning *to the same account* and *in the same asset*, are claims about how an execution unfolded; the transfers alone do not carry them.

Figure 1 shows the simplest case twice. In each panel, an externally owned account (EOA) invokes a smart contract (SC) that routes WETH through pools with different reserve ratios and recovers more than it sent. The two panels are one strategy routed differently: the intermediate USDT passes directly between pools in (a) and through the SC in (b), two transfers against four. The strategy is the same and the transfer graphs are not. Parallel paths that split and merge go further still: Figure 2 shows a real one, tx_R, the running example of the paper. These shapes recur across hundreds of pool contracts.

Detectors read the transfers and look for the shape. EigenPhi, the production MEV platform whose labels are the

Preprint. Under submission to a peer-reviewed security venue.

industry reference,[1] flattens a transaction into its transfer graph, extracts strongly connected components, and reports an arbitrage when the balance nearest the sender is positive [12]. Read this way, cases (a) and (b) are different objects though they are one strategy, and a withdrawal returning an asset to its owner is indistinguishable from a trade that profits (Appendix F-C; Section IV measures how often).

The ceiling is not specific to one tool. DeFiRanger [13], closest to our work, matches a hand-maintained catalog of attack patterns against a *cash flow tree*, with no formal guarantees. Graph-theoretic methods [14], [15], [16] enumerate cycles in aggregate token graphs at scale but collapse the call hierarchy separating a *swap* from a *relay*: alike in a flat graph, different in meaning. Machine-learning classifiers [17], [18], [19] and richer representations [20] produce labels without the chains that explain them. A survey [21] confirms the common crutch, protocol-specific knowledge, and that detectors degrade on unknown contracts [22], [23]. Missing is a *structural account* of what arbitrage *is* inside a trace.

Our key observation is that an execution trace admits a normal form, under which structural equivalence of fund flows is *decidable*. We turn each trace into an abstract syntax tree of token transfers and rewrite it, chaining, merging and annotating, until fixpoint. Rewriting invents nothing and terminates: the result carries exactly the transfers of the trace, reordered, with every account's balance unchanged whichever order the rules fire in. Our kernel scans the EVM-fixed execution order left to right, and under it the trace has a unique normal form.

Arbitrage detection is the demonstrating witness: cycles are never searched for, they *emerge*. If a set of transfers walks like an arbitrage, the system says so.[2] We claim soundness, not completeness, and state it of the transaction, not of our labels: when the system reports an arbitrage, that transaction's transfer graph contains a closed walk returning to its origin in a token-equivalent asset with strictly positive balance (Definition 7), naming neither the rewriting nor the normal form. The decoder uses only the standard ERC token and WETH ABIs, so designs reusing the `Transfer` signature need no protocol-specific decoding.

We contribute (i) the *substrate*, a rewriting system whose normal form makes structural equivalence decidable; (ii) a *sender-enriched AST*, in which each transfer carries a *sender* field σ derived from the call hierarchy that separates a swap from a relay without event catalogs; (iii) *Rocq proofs*, with zero admitted obligations, of preservation, termination, soundness over the transaction's own transfer graph, uniqueness and decidable equivalence; and (iv) *detection as the first query*, in which flash-loan arbitrages emerge structurally and verdicts carry their transfer chains, profit, and reasons.

Section IV evaluates the detector against EigenPhi and ArbiNet [19]. The Rocq sources, evaluation pipeline, and binaries are available at https://anonymous.4open.science/r/artifact-submission-2128.

[1]EigenPhi's public service was discontinued in June 2026 [11]; we compare against labels collected while it operated, which ship with our artifact (Section IV).

[2]After the duck test, attributed to James Whitcomb Riley.

II. Preliminaries

A. Ethereum Execution Model

Ethereum is a distributed state machine whose state is advanced by *transactions*. A transaction is signed by an *externally owned account* (**EOA**), an address controlled by a private key, and may invoke a *smart contract* (**SC**), a program deployed at a distinct address on the blockchain. Smart contracts can, in turn, invoke other contracts via internal calls (`CALL`, `DELEGATECALL`, `STATICCALL`), forming a nested call tree.

a) Execution trace: Replaying a transaction through the Ethereum Virtual Machine (EVM) tracer produces an *execution trace*: the ordered, hierarchical record of every internal call and its side effects. It preserves the nesting of the call tree and records, per frame, the caller, callee, call value, input and return data, and emitted event logs.

b) Token transfers: A *token transfer* is a movement of value from one address to another, and the trace records three forms: *native ETH*, as value attached to a `CALL` opcode; *ERC-20*, as `Transfer(from,to,amount)` event logs [24]; and *NFT*, as ERC-721 `Transfer` or ERC-1155 `TransferSingle`/`TransferBatch` events carrying a token identifier rather than a fungible amount (only fungible amounts contribute to profit). We treat them uniformly for cycle construction: a transfer is a tuple $t = (s, d, a, \tau, \sigma)$ where s is the source address, d the destination, a the amount or token identifier, τ the token type, and σ the *sender*: the address that initiated the nearest enclosing `CALL` frame in which the transfer event was emitted, derived from the call hierarchy of the execution trace. We write $s(t)$, $d(t)$, $a(t)$, $\tau(t)$ and $\sigma(t)$ for the five components of a transfer t. `DELEGATECALL` frames do not update σ (delegated code executes in the caller's context), so proxy contracts are handled correctly: σ reflects the external caller, not the proxy. σ is what separates a swap from a relay: in a swap both transfers share the external caller that orchestrated them, whereas in a relay the intermediary is itself the sender of the onward transfer. The transfers look alike; their senders do not.

c) Transaction costs: A transaction incurs a burned *base fee* (EIP-1559), a *priority fee* to the block builder, and optionally a direct contract-to-coinbase payment, used by MEV arbitrageurs to secure favorable ordering.

d) Automated market makers: An *automated market maker* (**AMM**) is a smart contract holding reserves of two or more tokens in a *liquidity pool* and pricing them algorithmically, without an order book. Each pool prices from its own reserves, so two pools over the same pair may offer different rates, creating an *arbitrage opportunity*: buy cheaply in one, sell for more in the other.

B. Transfer Graphs and Cash Flow Trees

We define the data structures and operators used in the algorithm and the proofs.

Definition 1 (Transfer graph)**.** *Given a transaction tx, its transfer graph $G = (V, E)$ is the directed multigraph whose vertices V are the addresses involved in tx and whose edges E are the transfers tx performs, one edge per transfer, each edge t directed from $s(t)$ to $d(t)$.*

Transfer graphs are flat: they record *what* was transferred, not the call hierarchy that produced it, and that hierarchy is what separates a round trip from a coincidence. The transaction of Appendix F-C makes this concrete. Its flat graph shows WETH leaving the contract and WETH coming back, and stops there; the call hierarchy shows the returning WETH to be the proceeds of two reward sales in frames of their own, which is what distinguishes repayment from gain. To keep that structure, we introduce the *cash flow tree*.

Definition 2 (Cash Flow Tree)**.** *A cash flow tree (CFT) over a transaction tx is defined inductively:*

- *a leaf* $\mathsf{Leaf}(t)$ *carries a single transfer t;*
- *a chain node* $\mathsf{Chain}(C)$ *carries a non-empty sequence C of transfers;*
- *a call node* $\mathsf{Tree}(v, [T_1, \ldots, T_m])$ *carries the address v whose code was executing and its children $T_1, \ldots, T_m$, themselves CFTs, ordered by their position in the execution trace.*

The CFT mirrors the EVM call stack: each internal `CALL` becomes a Tree node, each token transfer a Leaf, and a node's children are what occurred *within* that frame. Siblings were therefore produced by the same contract invocation, and that is the structure the rewriting exploits. The tree the decoder builds has leaves and call nodes only; chain nodes hold the sequences the rewriting assembles, so they appear once reduction begins. We call it an *abstract syntax tree* (**AST**), since the algorithm rewrites it syntactically rather than interpreting it as a graph.

The rewriting links sibling transfers into chains, then asks whether a chain closes on itself and pays. The remaining definitions make that precise, beginning with what a set of transfers does to an account.

Definition 3 (Balance)**.** *Let $t_1, t_2, \ldots, t_k$ be transfers. Their balance δ sends an address v and a token τ to the net signed amount that v receives in τ: each t_i carrying exactly token τ credits $d(t_i)$ and debits $s(t_i)$ by $a(t_i)$, and leaves every other address untouched. We write $\delta[v]$ when τ is clear from the context, and δ_C when the transfers are those of a chain C. The balance is gross: it accounts for these transfers and for nothing else, in particular not for execution costs.*

Definition 4 (Transfer chain)**.** *A transfer chain C is a sequence of transfers $t_1, t_2, \ldots, t_k$. It originates at $s(t_1)$ and terminates at $d(t_k)$, and its middleman set is $\{d(t_1), d(t_2), \ldots, d(t_{k-1})\}$: the addresses that relay tokens without being the origin or the final destination. The chain is connected when consecutive transfers meet, that is $d(t_i) = s(t_{i+1})$ for all $1 \le i < k$.*

Two chains C_1, C_2 with $d(C_1) = s(C_2) = j$ join at j under either token continuity, when the last token of C_1 is the first token of C_2, or balance continuity, when the junction is left short in no token: $BalCont(j) \equiv \forall \tau,\ \delta_{C_1}[j, \tau] + \delta_{C_2}[j, \tau] \ge 0$. Balance continuity is the weaker of the two.

We write $s(C)$, $d(C)$ and $M(C)$ for a chain's origin, destination and middleman set, and lift the token notation to chains: $\tau_{\mathrm{in}}(C)$ and $\tau_{\mathrm{out}}(C)$ are the tokens of t_1 and t_k, the assets the chain takes in and gives back, while $\tau_{\mathrm{mid}}(C)$ is the token of t_{k-1}, what the last intermediary passed on. For a two-transfer chain τ_{mid} and τ_{in} coincide; for longer ones they do not, and the rules below need both. In the implementation a chain is a binary tree whose in-order traversal is the sequence above, preserving the order of assembly. Closing a chain into a cycle requires matching tokens at both ends, but a chain may start with a native asset and end with its wrapped form.

Definition 5 (Token equivalence)**.** *Two token types τ_1, τ_2 are token-equivalent, written $\tau_1 =_\tau \tau_2$, when they are either identical or denote the same underlying asset through different representations (e.g., ETH and WETH). All other token pairs require strict equality. The relation is reflexive and symmetric. Transitivity is not required, as $=_\tau$ is checked only at cycle boundaries.*

The last two definitions say what the algorithm looks for. Both are stated over the transfer graph alone, so both can be checked against the transaction's own transfers.

Definition 6 (Cycle in G)**.** *Let v be an address. A cycle at v is a sequence of connected chains $C_1, \ldots, C_m$ with $m \ge 1$, whose concatenation $C = C_1 \cdots C_m$ satisfies*

1) *(maximal) no two consecutive pieces can be joined into one connected chain, so $C_1, \ldots, C_m$ is the decomposition of C into its longest connected runs;*
2) *(closed) C originates and terminates at v;*
3) *(drawn from the transaction) the transfers of C, counted with multiplicity, are a sub-multiset of E.*

When $m = 1$ the cycle is a single connected chain, the classical picture; a larger m means it closes through parallel legs, with $m - 1$ junctions where consecutive pieces fail to meet. The transaction of Appendix F-C illustrates the general case: its closed walks are cycles in this sense, and several close only through junctions where the token received differs from the token passed on.

Definition 7 (Arbitrage in G)**.** *A cycle C at v is an arbitrage in token τ when*

1) *(entry token) τ is the token of the first transfer of C;*
2) *(round trip in one asset) the first and the last transfer of C carry token-equivalent tokens;*
3) *(profit) the balance at the origin is strictly positive in that token, $\delta_C[v, \tau] > 0$.*

No cycle of the transaction in Appendix F-C is an arbitrage. Three carry token-equivalent tokens at both ends and so satisfy the first two conditions, but their pieces do not join: no walk over compatible tokens runs round, and the balance at the origin is zero. The same asset entering and leaving an address is an accounting fact, not a trade.

Definition 7 is gross by construction, hence checkable from the trace alone. Execution costs are not part of it: whether a cycle also gained after costs is a separate query on the algorithm's result. Requiring the round trip to close in one asset is the notion of cyclic arbitrage prior measurement work uses [14], [16]: a walk returning in a different token leaves the actor holding something else, and deciding whether that is a gain needs the price oracle this paper deliberately avoids.

C. Pipeline Overview

The pipeline has two layers. The *decode layer* ingests raw traces (`debug_traceTransaction` or a pre-indexed database). Transfer extraction uses only the standard ERC token and WETH signatures; Sourcify ABIs and the 4byte directory serve call-name and OSINT enrichment, which the fixpoint and the validation never consume. It is the only stage touching external databases. The *analysis layer* is pure and in-memory: it builds the tree of Definition 2, rewrites it, computes balances, and classifies.

III. Normalization and Detection

Definition 7 says what we are looking for. Finding it by searching the transfer graph means enumerating cycles in a structure that has already lost the call hierarchy, which is what lets a chain of transfers that merely passes through an address look like one that returns to it. We work on the tree instead, rewriting it until the cycles appear as subterms.

Every object a rule touches is a cash flow tree (Definition 2): a leaf carrying one transfer, a chain node carrying a labelled sequence, or a call node carrying an address and its ordered children. A rule rewrites the children of one node and yields a tree of the same kind. The label records what the reduction has established about a chain: CHAINING for a sequence assembled from adjacent transfers, MERGING for one assembled from parallel branches, BURN and MINT for sequences ending at or starting from the null address, CYCLE for a closed chain that returns in a different asset, and ARB for one that returns in the asset it left in.

The rules derive from the chain's own conventions (swap pairing, null-address mint and burn, wrapping) and from the composition of walks; R5 is the sole deployment hint. The reduction has two rewriting stages, grouped in Table I by *locus* rather than by operation: both stages chain and both merge. *Leaf manipulation* (R_1–R_{10}) fires on siblings within one call frame; when no rule applies at a level, its chains and leaves are *lifted* into the enclosing frame, becoming siblings of the call that produced them, and reduction resumes there. *Node manipulation* (R_{11}–R_{13}) fires once lifting has put operands from different frames side by side. Each node rule is the cross-frame counterpart of a leaf rule with a stricter guard (R11 of R4, R12 of R6, R13 of R7), stricter precisely because lifting has destroyed the frame evidence the leaf rule could rely on. Neither stage names a query, and neither adds nor drops a transfer. The *annotation* rules (R_{14}, R_{15}) fire within both stages, and are where the word *arbitrage* first appears: a chain whose endpoints coincide becomes ARB when it also leaves and returns in token-equivalent assets, and CYCLE otherwise. Annotation is structural and does not consult amounts, so *validation* (R_{16}) runs once after the fixpoint and revokes the ARB label wherever the balance at the origin is not positive.

We describe the algorithm through a real Ethereum transaction tx_R[3] that splits a payment across parallel paths and recombines them, and that EigenPhi does not flag as an arbitrage. Figure 2 shows its transfer graph: the SC splits 0.0575 WETH into three parallel paths through six pools, each converting an intermediate token into BEAN, which converges on a single BEAN/WETH pool that returns 0.0598 WETH (profit: $+0.0023$ WETH).

A. From Traces to ASTs

Before the stages begin, the AST of Definition 2 is built from the decoded trace: one Tree node per call frame, one Leaf per value-movement event (`Transfer`, `TransferSingle`, `TransferBatch`, `Mint`, `Burn`, `Deposit`, `Withdrawal`, native ETH), with σ taken from the enclosing frame as in §II-A. Non-value events such as `Approval` are discarded. Each decoded transfer becomes exactly one leaf, so the tree carries all of them and no others, and the nesting is the call hierarchy. That the trace admits this reading at all rests on a design invariant of blockchain virtual machines:

Property 1 (Deterministic sequential execution)**.** *Let tx be a transaction executed on a blockchain in state S. The execution trace $\mathcal{T}(tx, S)$ satisfies:*

1) ***Determinism.*** *$\mathcal{T}$ is a function: the trace is uniquely determined by (tx, S).*
2) ***Sequential order.*** *Within each call frame, instructions execute in program order. No concurrent or out-of-order execution occurs within a frame.*
3) ***Tree structure.*** *Nested calls (`CALL`, `DELEGATECALL`, `STATICCALL`) create child frames. The resulting call hierarchy is a rooted, ordered tree.*

None of the three is an empirical observation: consensus requires deterministic state transitions, sequential order within a frame follows from the stack-machine architecture, and the tree structure from the call/return discipline. A machine violating any of them could still reach consensus, as parallel-execution VMs do by scheduling conflict-free frames concurrently, but not under the ordered-tree view we exploit. EVM-compatible chains satisfy Property 1 by construction, and it is the only assumption our results make about the execution environment; we validate on two further EVM chains (Appendix G). Non-EVM machines are future work.

a) Trimming: Trimming then removes structure that carries no transfer. A Tree node whose children are all non-transfer events is pruned; a node with exactly one child is collapsed into that child; and any subtree whose recursive pruning yields no Leaf is removed. A second cleanup drops degenerate leaves, transfers of zero amount with $\sigma = s(\ell)$,

[3] `0x275f9642556a58802eafdd8289aa19a7275e9d40962056095bb9b5c51ac3d246`

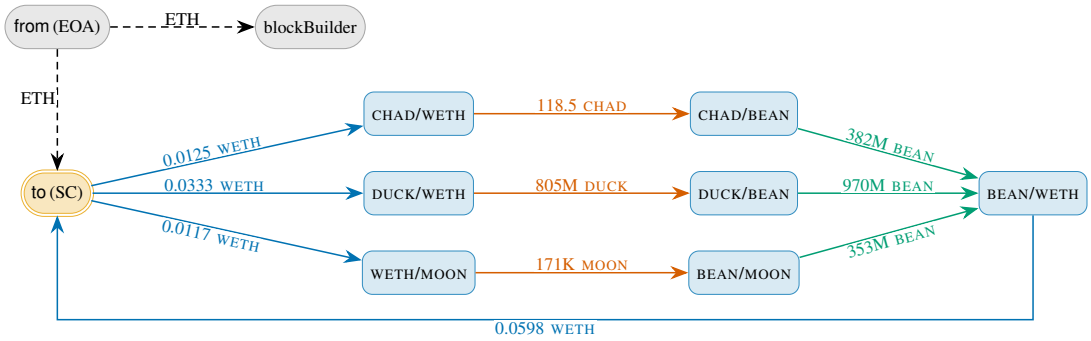

Fig. 2. Transfer graph of tx_R. Three parallel paths through six pools; dashed edges are cost transfers.

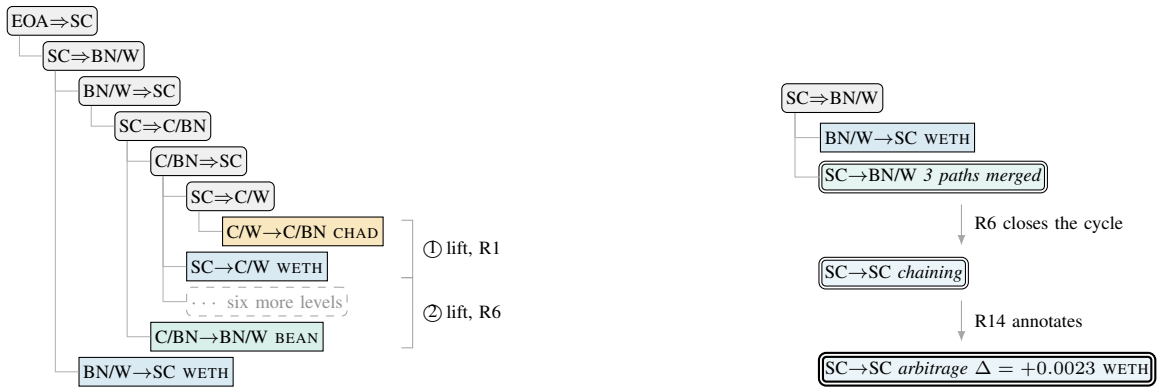

(a) The trimmed tree, drawn down the CHAD path only. ⇒ is a call frame, → a transfer; the dashed node elides the rest.

(b) After the structural fixpoint's merge: R6 closes the aggregate, R14 annotates it, and validation confirms a positive balance at the origin.

Fig. 3. Reduction of tx_R, a callback cascade in which lifting creates every chaining opportunity. Double borders mark chains.

which move no value and would otherwise block chaining at the shared address. Construction and trimming together produce the tree T_0 on which the stages operate. Every guarantee in §III-F is stated from T_0: the theorems say what the rewriting does to the transfers it is given, not whether those transfers faithfully reflect the value that moved: that fidelity is the decode layer's, and belongs to the trusted base (§VI). For tx_R the raw trace holds fifty-one call frames, which trimming collapses to twelve. The shape survives: each pool calls back into the SC before settling, so the frames nest twelve deep and each of the ten route transfers sits alone in its own frame, none adjacent to another (Figure 3(a)). The two dashed transfers of Figure 2 are native-ETH costs and never enter T_0; the profit query accounts for them after the fixpoint (§III-D). Panel (b) follows the reduction from there.

B. Stage 1: Leaf Manipulation

Leaf manipulation, the first rewriting stage (R1–R10), operates on sibling children within each Tree node, bottom-up from the deepest subtrees to the root. Algorithm 1 gives the pseudocode, Table I the rules.

a) Chaining: Two sibling leaves are *chainable* when $d(\ell_1) = s(\ell_2)$ and $\tau(\ell_1) \neq \tau(\ell_2)$ (R1). The address match locates a shared intermediary, typically a pool; the token mismatch is what a swap looks like from outside, one asset in

function MANIPULATE-LEAVES(T):
  for each level ℓ from deepest to root **do**
    repeat
      for each sibling pair (ℓ_i, ℓ_{i+1}) at level ℓ
        if $d(\ell_i) = s(\ell_{i+1})$ and $\tau(\ell_i) \neq \tau(\ell_{i+1})$
        then replace (ℓ_i, ℓ_{i+1}) with CHAIN(ℓ_i, ℓ_{i+1})
      for each Tree$(c, [t_1 \dots t_m])$ at level ℓ
        if all t_j are chains or leaves
        then lift $t_1 \dots t_m$ to parent
    until no change at level ℓ
  return T

Algorithm 1. Leaf manipulation. CHAIN constructs a transfer chain from two adjacent transfers. Lifting dissolves fully-reduced Tree nodes.

and another out. The pair becomes a chain with origin $s(\ell_1)$, destination $d(\ell_2)$ and middleman $\{d(\ell_1)\}$. The rule extends transitively, to a chain and an adjacent leaf (R6) and to two chains that meet (R10); R10 also fires under balance continuity at the junction (Definition 4), which admits balance-preserving routing such as a WETH↔USDC relay.

Chains that run in parallel rather than in sequence are merged instead. R7 takes two chains with the same origin and destination that give back the same asset but pass through different intermediaries: the premise $\tau_{\text{mid}}(C_1) \neq \tau_{\text{mid}}(C_2)$

TABLE I

REWRITING RULES. ℓ: LEAF; C_{label}: LABELLED CHAIN. †OPTIONAL DEPLOYMENT HINT.

#	Premise	Conclusion
Leaf manipulation (within a call-frame node)		
R1	$d(\ell_1){=}s(\ell_2)$, $\tau(\ell_1){\neq}\tau(\ell_2)$, $burn(\ell_1){\Leftrightarrow}mint(\ell_2)$	$(\ell_1,\ell_2) \to C_{chain}$
R2	ℓ_b burn, ℓ not mint, $d(\ell_b){=}s(\ell)$	$(\ell_b,\ell) \to C_{burn}$
R3	ℓ_m mint, ℓ not burn, $d(\ell){=}s(\ell_m)$	$(\ell,\ell_m) \to C_{mint}$
R4	$d(\ell_1){=}s(\ell_2)$, $d(\ell_2){=}s(\ell_1)$, $\tau(\ell_1){=}\tau(\ell_2)$, $d(\ell_1) \notin Routers$, $\exists\, i,\ \sigma(\ell_i){\neq}d(\ell_1)$	$(\ell_1,\ell_2) \to C_{chain}$
R5†	$d(\ell_1){=}s(\ell_2)$, $\tau(\ell_1){=}\tau(\ell_2)$, $d(\ell_1) \in Routers$, $burn(\ell_1){\Leftrightarrow}mint(\ell_2)$	$(\ell_1,\ell_2) \to C_{chain}$
R6	$d(C){=}s(\ell) \vee d(\ell){=}s(C)$	$(\ell,C) \to C'_{chain}$
R7	$s(C_1){=}s(C_2)$, $d(C_1){=}d(C_2)$, $s{\neq}d$, $\tau_{\text{out}}(C_1){=}\tau_{\text{out}}(C_2)$, $\tau_{\text{mid}}(C_1){\neq}\tau_{\text{mid}}(C_2)$	$(C_1,C_2) \to C_{merge}$
R8	$s(C_1){=}s(C_2){=}d(C_1){=}d(C_2)$, $[\tau_{\text{in}}(C_1){=}\tau_{\text{in}}(C_2) \wedge \tau_{\text{mid}}(C_1){=}\tau_{\text{mid}}(C_2) \wedge \tau_{\text{out}}(C_1){=}\tau_{\text{out}}(C_2)] \vee BalCont(s)$	$(C_1,C_2) \to C_{merge}$
R9	$s(C_1){=}d(C_1){=}s(C_2){=}d(C_2)$, $\tau_{\text{in}}(C_1){=}\tau_{\text{in}}(C_2)$, $\tau_{\text{out}}(C_1){=}\tau_{\text{out}}(C_2)$	$(C_1,C_2) \to C_{merge}$
R10	$d(C_1){=}s(C_2)$, $[\tau_{\text{out}}(C_1){=}\tau_{\text{in}}(C_2)] \vee BalCont(d(C_1))$	$(C_1,C_2) \to C_{chain}$
Node manipulation (across call frames)		
R11	$d(\ell_1){=}s(\ell_2)$, $\tau(\ell_1){=}\tau(\ell_2)$, $d(\ell_2){\neq}s(\ell_1)$, $d(\ell_1) \notin Routers$, $\sigma(\ell_1) \neq d(\ell_1)$	$(\ell_1,\ell_2) \to C_{chain}$
R12	$[d(C){=}s(\ell) \wedge \tau_{\text{out}}(C){=}\tau(\ell)] \vee [d(\ell){=}s(C) \wedge \tau(\ell){=}\tau_{\text{in}}(C)]$	$(\ell,C) \to C'_{chain}$
R13	R7's premises, and $\tau_{\text{in}}(C_1){=}\tau_{\text{in}}(C_2)$	$(C_1,C_2) \to C_{merge}$
Annotation (both leaf and node stages)		
R14	$s(C){=}d(C)$, $\tau_{\text{in}}(C){=}_{\tau}\tau_{\text{out}}(C)$, $[\sigma(C){\notin}C \vee s(C){=}\sigma(C)]$, $\neg\, WrapUnwrap(C)$	$C_{chain} \to C_{arb}$
R15	$s(C){=}d(C)$, $\sigma(C) \in C$	$C_{chain} \to C_{cycle}$
Validation (post-annotation)		
R16	$\delta_C[s(C), \tau_{\text{in}}(C)] \leq 0$	$C_{arb} \to C_{cycle}$

says exactly that, and without it the rule would merge a route with itself. R8 and R9 are its closed forms, for chains that already return to their origin, R8 requiring the intermediate token to agree as well so that merging is summation. A merged node is labeled *merging* rather than *chaining*: a chained node extends one path, a merged node holds several. Either way the delta maps add, $\delta_{C_m}[v,\tau] = \delta_{C_1}[v,\tau] + \delta_{C_2}[v,\tau]$ (Definition 3).

Chaining a round trip needs one further decision. When two sibling leaves return to where they started through an address B (R4), B is either swapping, in which case the pair is a chain, or merely relaying, in which case chaining it would short-circuit the path. We read this off the *sender* field: when $\sigma \neq B$ on either leaf, an external contract is driving the interaction *through* B, the structural signature of a swap. The check needs no external metadata, only the call hierarchy already in the trace. R4 yields a plain chain; whether the round trip deserves a name is decided later, by annotation. Deployments may optionally declare router addresses (R5, the only protocol-specific rule) so that same-token transfers through an aggregator chain anyway; disabling the hint costs recall on universal-router transactions and adds no false positives, since removing a rule only removes reductions. Ours holds one address, the Uniswap V4 universal router.

function ANNOTATE-AND-REDUCE(T, *from*, *to*):
  // Label closed chains (Def. 6)
  $T' \leftarrow$ ANNOTATE-CYCLES(T, *from*)
  // Merge complementary open chains
  $T'' \leftarrow$ CONNECT-CYCLES(T', *from*, *to*)
  if $T'' = T$ **then return** T
  else return ANNOTATE-AND-REDUCE(T'', *from*, *to*)

Algorithm 2. Annotation and connection loop; runs after the structural fixpoint.

b) Mint- and burn-aware chaining: A transfer out of the null address (`0x0000...0`) is a *mint* and one into it a *burn*; the decode layer normalizes both to name the emitting contract instead. Since the null address is not a participant, neither can chain on its own, so each pairs with an adjacent ordinary transfer that completes the flow. A burn followed by a transfer out of the same contract is a *token burn* (R2), value leaving as the token is destroyed, which also covers Withdrawal + NativeTransfer (unwrap); a transfer followed by a mint is the mirror (R3), covering Deposit + NativeTransfer (wrap). The two exclude each other, so neither fires on a burn feeding a mint, a token migration rather than either, which R1 chains plainly. Token burns and mints then take part in cycle connection on the same footing as *cycle*-labeled chains, so the fixpoint reaches arbitrages routed through wrapped-token contracts and vault deposits. The normalization belongs to the decode layer; the algorithm treats the label as opaque.

c) Lifting: Once an internal Tree node holds only chains and leaves, its children are *lifted* into the parent, becoming siblings of the frame that produced them. This exposes transfers hidden inside nested calls for chaining one level up. Only internal frames are lifted; the root is never dissolved.

d) Bottom-up iteration: Chaining and lifting run as a fixpoint at each level, deepest first. In tx_R lifting is not housekeeping but the precondition for everything else: in Figure 3(a) no two of the ten transfers are siblings, so no rule can fire at all until frames are dissolved. The WETH leaf $SC \to C/W$ sits beside the frame holding $C/W \to C/BN$ in CHAD; one lift makes the two leaves siblings and R1 chains them into $SC \to C/BN$ (mark ①). A second lift brings the BEAN leaf $C/BN \to BN/W$ alongside, and R6 extends the chain to $SC \to BN/W$ (mark ②). Twelve levels of this leave three chains agreeing at both boundaries but differing in the middle (τ_{mid} = CHAD, DUCK, MOON) beside the return leaf $BN/W \to SC$, ready for the merge.

C. Stage 2: Node Manipulation

After leaf manipulation, the root Tree node's children are a mixture of transfer chains (Definition 4) and residual Leaf nodes. We write $a \in C$ for $a \in M(C)$. The node-level pass first chains residual elements using a *same-token* rule (R11), the dual of the leaf-level different-token rule: it captures the same asset flowing across contract boundaries. Likewise, a leaf and a chain are chained when address-adjacent and token-compatible (R12). Each address absorbed this way joins

the chain's middleman set M; in practice these are routers, aggregators and proxies, recognized structurally from the pass-through pattern rather than from any list. Parallel chains are merged as at the leaf level, by R13: R7's premises with the entry tokens pinned as well, which the node level can require because both origins are frame actors and their entry tokens are therefore determined. The annotation rules (R_{14}, R_{15}) then label the chains that close. Algorithm 2 gives the pseudocode and Table I the rewriting rules.

a) Cycle annotation: Cycle annotation labels each closed chain ($s(C) = d(C)$) with one of two labels (R14–R15). Let $\sigma(C)$ be the σ of the leaf at $s(C)$; when ambiguous, $\sigma(C)$ is taken from the eldest ancestor frame covering the operands, so that σ tracks the call frame that authored the chain rather than the bottom-up trace order. The two rows part on $\sigma(C)$: R14 wants it outside the middleman set (a bot orchestrating swaps) or equal to the origin (an EOA-initiated cycle), R15 finds it inside, which is routing rather than profit extraction. R14's remaining guard excludes pure native/wrapped roundtrips: $WrapUnwrap(C)$ holds when $M(C)$ contains a contract of $\tau_{\text{in}}/\tau_{\text{out}}$ and both sub-chains are leaves or both satisfy it. Annotation does not inspect the delta map; the economic check is R_{16}'s (§III-D).

b) Cycle connection: Not all cycles form within a single subtree: a transaction may leave two labeled chains that close only when taken together, one carrying the outward leg and one the return. The *cycle connection* rule identifies pairs of already-labeled chains C_1, C_2 (labeled *cycle*, *token burn*, or *token mint*) at the same tree level such that (i) $s(C_1) = s(C_2) = to$ (same origin, equal to the transaction recipient), (ii) $\tau_{\text{out}}(C_1) = \tau_{\text{in}}(C_2)$ (complementary token flows), and (iii) $s(C_1 \cdot C_2) = d(C_1 \cdot C_2)$ (the concatenation forms a cycle). An additional filter excludes pairs where either chain's middleman set is reduced to the sender alone ($M(C_i) = \{\sigma(C_i)\}$): a routing pattern (cf. R15). When such a pair is found, the two chains are merged into a single cycle node. Connection uses strict token equality; annotation uses $=_\tau$ (Definition 5) to label the resulting cycle. This separation is deliberate: connection matches exact token flows, while annotation recognizes that a native-asset transfer followed by a wrapped-asset chain (or vice versa) closes the same economic cycle. $=_\tau$ is a representation-level fact about the chain, not about any specific protocol.

c) Termination: Each pass of ANNOTATE-AND-REDUCE either (i) labels at least one chain as *arbitrage* or *cycle*, or (ii) merges two distinct chains into one, strictly reducing the child count of some Tree node. Since labels are monotonic (a chain is never re-labeled from *arbitrage* back to *chaining*) and the node count is finite, the loop terminates in at most $3n - 2$ passes, where n is the initial number of Leaf nodes (Theorem 2). That bounds *passes*; what a pass costs is an implementation matter, priced and measured in §IV-G. Deep, narrow trees converge fast because each subtree is small; wide, flat ones approach the pass bound.

In tx_R the three chains left by the leaf stage share origin SC and destination BN/W and agree in both boundary tokens, so R13 merges them into one aggregate, and the return leaf $BN/W \rightarrow SC$ closes that aggregate into a cycle by R6. Both fire in the structural fixpoint, which runs the rules of *both* loci to exhaustion (a merge creates new adjacencies, and chaining consumes them) before any label is assigned. Algorithm 2 is the loop that follows: here it only names the cycle (Figure 3(b)).

function DETECT-ARBITRAGE(*trace*, *from*, *to*, *meta*):
  // Build (§III-A)
  $T \leftarrow$ TRIM(BUILD-AST(*trace*))
  // Both loci (§III-B, §III-C): R_1–R_{13}
  $T \leftarrow$ STRUCTURAL-FIXPOINT(T)
  // Annotation (§III-C): R_{14}, R_{15}, connection
  $T \leftarrow$ ANNOTATE-AND-REDUCE(T, *from*, *to*)
  // Validation (§III-D): R_{16}
  $T \leftarrow$ VALIDATE-DELTAS(T, *to*)
  // Profit (§III-D), verdict (§III-E)
  $(C, L) \leftarrow$ EXTRACT-AND-RECOVER(T, *to*)
  $\Delta \leftarrow$ PROFIT(C, L, *to*, *meta*)
  return CLASSIFY(C, L, Δ)

Algorithm 3. Complete detection pipeline.

function CLASSIFY(C, L, Δ):
  $R \leftarrow \emptyset$ // reason accumulator
  if $C = \emptyset$ **then** $R \leftarrow R \cup \{\text{NO_CYCLES}\}$
  if Δ_{gross} is mixed **then** $R \leftarrow R \cup \{\text{BALANCE_MIXED}\}$
  if net profit ≤ 0 **then** $R \leftarrow R \cup \{\text{NEG_PROFIT}\}$
  if Δ_{net} is mixed **then** $R \leftarrow R \cup \{\text{FINAL_MIXED}\}$
  if Δ_{net} is negative **then** $R \leftarrow R \cup \{\text{FINAL_NEG}\}$
  if $L \neq \emptyset$ **then** $R \leftarrow R \cup \{\text{LEFTOVERS}\}$
  // Verdict (strict priority)
  if NO_CYCLES $\in R$ **then return** (*None*, R)
  if LEFTOVERS $\in R$ **then return** (*Warning*, R)
  if FINAL_NEG $\in R$ **then return** (*Warning*, R)
  if FINAL_MIXED $\in R$ **then return** (*Warning*, R)
  return (*Arbitrage*, R)

Algorithm 4. Classification logic.

D. After the Fixpoint: Validation and Profit

Once the fixpoint terminates, the reduced AST contains annotated cycles, open transfer chains that did not close, and residual Leaf nodes, the transfers the reduction could not place, which we call *leftovers*. Validation (R_{16}) runs once on that result, after which a profit figure and a verdict are read off. Algorithm 3 gives the complete pipeline, writing STRUCTURAL-FIXPOINT for the reduction of §III-B and §III-C, which iterates Algorithm 1 and the node rules of Table I until neither locus applies; Algorithm 4 details the classification logic, with $\Delta_{\text{gross}}[\tau] = \sum_C \delta_C[s(C), \tau]$ and $\Delta_{\text{net}} = \Delta_{\text{gross}} - gas$, the costs charged against the component they are denominated in; "mixed" = opposite-sign components. The two negative conditions of Algorithm 4 differ in scope: NEG_PROFIT tests that one component, FINAL_NEG tests them all.

a) Delta validation: VALIDATE-DELTAS applies R_{16} to every chain labeled *arbitrage*: it reads $\delta_C[s(C), \tau_{\text{in}}(C)]$ and

downgrades the label to *cycle* when that entry is not positive, so that no structurally valid but unprofitable cycle reaches the profit calculation as an arbitrage. It runs here rather than inside annotation because a chain's delta is complete only once every sub-chain connected to it has contributed. When the transaction sender and receiver coincide (self-call), VALIDATE-DELTAS is skipped: the contract is both origin and intermediary of every cycle, making per-cycle delta attribution unreliable.

b) Leftover transfers: EXTRACT-AND-RECOVER first extracts all transfers from the reduced AST that were not incorporated into an arbitrage cycle or a transfer chain. These *leftovers* indicate that the reduction could not reconstruct a complete flow path for those transfers. The two dominant causes are missing transfer decodings (non-standard mechanisms invisible to the decoder) and complex routing that pairwise chaining cannot resolve. Leftovers are recorded alongside the detected cycles; their presence signals that the profit calculation may be incomplete.

c) Leftover cycle recovery: Before computing the final profit, a two-pass recovery step attempts to extract additional cycles from the leftovers.

First, it identifies *specular pairs*: two leftover transfers (A, B, a, τ) and (B, A, a, τ) with matching token, matching amount, and reversed endpoints. These are exact round-trips, characteristic of flash-loan borrow/repay and other same-amount refund patterns. Specular pairs are removed from the leftover list and grouped into *leftover cycles*. Their net delta for the loan token is zero (the exact borrow amount is returned); the arbitrageur's profit is captured separately by the AST cycles that used the borrowed funds.

Second, remaining leftovers are scanned for *complementary transfers*: two transfers involving the same token τ where either endpoint connects ($A = B'$ or $B = A'$), regardless of amount. These capture partial round-trips where the repayment differs from the borrowed amount (e.g., a flash loan with a fee). Complementary groups are merged into leftover cycles and their net delta is added to the accumulator. Remaining unmatched transfers stay as leftovers in the final output.

This two-pass recovery is where lending-based arbitrages are captured: the borrower takes a flash loan on one side of the call tree and repays it on the other, too far apart for the chaining rules to connect. Specular and complementary recovery reconstruct these round-trips from the leftovers.

d) Profit calculation: PROFIT computes the net token balance of address to from the cycles and leftovers produced by EXTRACT-AND-RECOVER. Each chain carries the balance δ_C of Definition 3, maintained as it is assembled; for a cycle rooted at to, the entry $\delta_C[to, \tau]$ is the gross profit in τ before costs. Any remaining leftover transfer whose destination is to is also added to the balance, capturing direct incoming value that was not part of a cycle.

Three cost components are then deducted: (i) the *base fee* $gas_used \times base_fee$ (burned by the network); (ii) the *priority fee* $gas_used \times (effective_gas_price - base_fee)$ (tip to the block builder); and (iii) an optional *direct builder payment* $\mathsf{Leaf}(to, builder, a, \mathrm{ETH})$ to the builder's coinbase, common in MEV strategies. The first two are read from the transaction's own metadata, not from the tree, which is why the native-ETH cost edges of Figure 2 never had to enter T_0. The third is an ordinary leaf, and the walk that collects it sets it aside rather than counting it as profit or as a leftover, so paying the builder does not by itself make a transaction inconclusive. The result is a set of per-token net balances Δ after all costs.

e) Why profit is attributed at to: The rewriting is indifferent to who profits: it closes a cycle wherever one closes, and a cycle rooted at an inner contract is annotated like any other. The cost side is what does not generalise. Gas is paid once, by the sender, for the transaction as a whole, and no principled share of it belongs to an inner address that happens to net positive; without that share there is nothing to weigh a positive inner balance against, and a verdict there would report a gross figure as though it were net. We therefore attribute only where the accounting closes, and leave cycles at inner addresses detected but unclassified. The choice costs recall and never soundness, and §IV measures what it leaves behind.

E. Classification

Classification inspects Δ along sign and token diversity, yielding four cases: *positive single-token* ($|\Delta|{=}1$, $a{>}0$), *positive multi-token* ($|\Delta|{>}1$, all $a_i{>}0$), *mixed* ($|\Delta|{>}1$ with differing signs, e.g. $+0.5\,\mathrm{WETH}$, $-200\,\mathrm{USDT}$), and *negative* ($|\Delta|{=}1$ with $a{\leq}0$, or $\Delta{=}\emptyset$). This classification is computed twice: once on the gross balance (before costs) and once on the net balance (after costs). CLASSIFY (Algorithm 4) turns the six resulting conditions into a verdict accompanied by an ordered list of *reasons*, diagnostic labels that explain the decision to the analyst. Only four of the six gate the verdict: a transaction is classified *Arbitrage* when a cycle survived validation, no leftovers remain, and the *net* balance is positive in every component. When any of the four is uncertain, the verdict conservatively falls back to *Warning*, and the gross-balance and net-profit conditions report without deciding.

a) Token equivalence: R14 tests $=_\tau$ (Definition 5), so a cycle that leaves in a native asset and returns in its wrapped form is labeled *arbitrage* and is covered by Theorem 3. The mechanization leaves $=_\tau$ an arbitrary boolean relation on tokens: no proof invokes any algebraic property of it, so soundness holds for every instantiation, and the reflexivity and symmetry a deployment will want are stated as an obligation on that deployment rather than assumed anywhere.

For tx_R, the three parallel paths (Figure 2) reduce to the single arbitrage cycle of Figure 3(b), spanning all seven pools, with no leftovers and $\Delta_{\mathrm{gross}} = \{(\mathrm{WETH}, +0.0023)\}$. Costs leave $\Delta_{\mathrm{net}} = \{(\mathrm{ETH}, +5.5 \times 10^{-5})\}$, reported in the native asset because the deployment treats it and its wrapped form as equivalent (Definition 5): one component, positive, so none of the four gates fires and the verdict is *Arbitrage*.

A verdict of *Arbitrage* certifies closure and token match from annotation, positivity from validation, and that every *decoded* transfer is accounted for; Theorem 3 states the guarantee precisely.

b) Warnings as diagnostic signals: A *Warning* means the system cannot confirm with full confidence, typically because leftovers indicate incomplete decoding or because a mixed-sign Δ requires cross-token valuation we deliberately avoid. The reasons in R are split into *verdict-determining* (NO_CYCLES, LEFTOVERS, FINAL_NEG, FINAL_MIXED) and *explanatory* (all others). Only the former gate the decision; the latter provide a forensic diagnostic picture.

F. Formal Properties

Five statements say what the rewriting may do to a trace, and therefore what a verdict is worth. Each is stated in English first and formally second, proved against the sixteen rules of Table I, and assumes Property 1 and nothing further about the execution environment. Proofs are in Appendix D, which opens by separating what is mechanized from what is not (Table III).

The reduction re-brackets the transfers it is given. It drops none, duplicates none, and invents none, so every balance stays exactly where the trace put it, whichever order the rules fire in.

Theorem 1 (Preservation)**.** *Let T_0 be the initial AST and T_f any tree reachable from it. Every chain of T_f tracks walks in G (Definition 1); every transfer of T_f is a transfer of T_0; and T_0 and T_f carry the same multiset of transfers.*

The reduction also stops, and stops soon. Two counters fall as it runs: the chains still unlabelled, u, and the total number of children, c. In the annotation-and-connection loop neither rises and every non-trivial pass consumes a unit of their sum, which on a fully lifted non-empty input takes the arithmetic form $3n - 2$, the bound on passes. The unrestricted relation ranks trees by (c, u) instead, which every rule decreases (Appendix D). Lifting is not needed to terminate, only to give the budget its arithmetic form.

Theorem 2 (Termination)**.** *The deterministic annotation-and-connection fixpoint reaches a normal form from every reduced AST. If its input is fully lifted and non-empty with n transfers, it takes at most $3n - 2$ passes. The full rewriting relation is well-founded under arbitrary rule orders.*

Soundness is the statement the rest of the paper is written to support, so it is worth being exact about what it does and does not say. It concludes about the transaction, not about our labels: when the pipeline answers *Arbitrage*, the transaction's own transfer graph contains an arbitrage in the sense of Definition 7, a definition that names neither the rewriting, nor the normal form, nor any label the reduction assigns.

Theorem 3 (Soundness)**.** *Let T_0 be a decoded trace and T_f any tree reachable from it. If* CLASSIFY *returns Arbitrage on T_f and at least one cycle survives R_{16} and the net-positive gate, then there are an address v, a token τ and a bundle of walks over the transfers of T_0 that together form an arbitrage at v in τ (Definition 7).*

Its two structural hypotheses hold of any decoded trace. The third is validation itself, stronger than Definition 7 needs (Appendix D); the fixpoint path discharges it by construction, since validation runs before the cycles are read off. The one path that can report *Arbitrage* without a surviving cycle is the post-fixpoint promotion of §IV: 0.8% of detections, the only component outside the mechanized core.

Sketch. Three steps, of which only the second has content. (i) Reading the verdict backwards is mere inversion: *Arbitrage* requires a chain of T_f carrying the ARB label that R_{16} did not revoke. (ii) By Theorem 1 the reduction can neither manufacture nor duplicate a transfer, so that chain's transfers are transfers of T_0, counted with multiplicity. This is the bridge, and what makes the conclusion a claim about the transaction rather than a restatement of how we labelled it. (iii) Closure, token match and a positive balance at the origin are read off the chain and transfer verbatim to G, and its maximal decomposition into connected runs is the bundle Definition 7 asks for. □

Two consequences follow. Every balance the system reports is a balance of the input trace, so a profit figure cannot be an artefact of the reduction. And Definition 7 is not satisfied by anything merely circular: a two-leg swap leaving in one asset and returning in another meets every other clause and is rejected on the round-trip condition alone, which we check as a mechanized counterexample.

Convergence is where the execution model earns its keep. Left free, the rules can be applied in many orders; the kernel fixes one, scanning the EVM's trace order left to right, and under it the answer is unique.

Theorem 4 (Uniqueness)**.** *Under the deterministic kernel over the execution's trace order, every AST has a unique normal form. Under* every *order, any two reachable trees agree on the balance $\delta[v, \tau]$ at every address v and token τ. On well-formed trees, two one-step divergences are joinable up to reassociation of parallel merges, the same branches grouped differently.*

The three clauses answer three different questions, and only the first is about syntax. Well-formedness is linearity, pairwise-distinct trace positions, which decoded trees have by construction and every rule preserves, plus a frame condition at the divergence site (Appendix D). Whether local joinability extends to a global statement is work in progress; every result in this paper uses the deterministic order and is unaffected either way.

Theorem 5 (Decidability)**.** *Under the deterministic kernel, two ASTs are joinable if and only if their kernel normal forms are equal, and equality of those normal forms is decidable. The coarser equivalence that identifies trees differing only by reassociation of parallel merges is decidable as well.*

Preservation and termination follow the two counters above by induction on rule applications. Uniqueness follows because the step function is total, so at most one rewrite fires per

tree. Decidability follows from uniqueness, a terminating computation of normal forms, and structural comparison. For a terminating confluent rewrite system the word problem is classically decidable [25], [26], [27], [28]; here it follows instead from termination, the deterministic kernel, and structural comparison of normal forms.

a) What is certified, and what is trusted: The five theorems are mechanized in Rocq: 13 501 lines, 432 lemmas, 13 corollaries and one worked counterexample, with no admitted obligation and no added axiom. The development declares eleven parameters, among them the address and token types, token equivalence, the burn and mint predicates, and the router hint of R5. They are declared and never defined, and no proof assumes anything about them beyond their types, so the theorems hold for every instantiation a deployment chooses. Two well-formedness conditions are stated but deliberately never assumed, the reflexivity and symmetry of $=_\tau$ among them; they are obligations on the deployment, not hypotheses of the results. Appendix D maps each theorem to its mechanized statement.

b) Specification and implementation: The system in production is OCaml, and the mechanized rules mirror it one for one: each rule of Table I is a constructor, and the mechanized kernel implements the same priority policy as the production module. That *kernel* is extractable, and the extracted module compiles and runs with placeholder realizers for the declared parameters, so the specification is executable rather than merely readable. What we have not done is differential testing of the two at trace scale; we commit to it, and until then their correspondence is a matter of construction and review, not measurement. Property 1 is not assumed anywhere: it is encoded in the data structure, since the tree of Definition 2 has ordered children, which is exactly what the property guarantees.

G. Implications of Decidability

Theorem 5 makes the normal form a substrate rather than an answer: any decidable predicate over normal forms is a query, and detection is only the first of them. Exact structural equivalence is the second, deciding whether two transactions reduce to the same form; a coarser *family* equivalence is the third, composing that test with a skeleton map sk that erases path lengths, arities and token identities, so a three-arm and a five-arm star fall together. Each composes normalization with a decidable test on trees, so each is decidable and linear in the size of the normal form: under sk, tx_R becomes $\mathsf{Star}(\star, \mathsf{Swap}(\star,\star), \star)$, as does any multi-arm star with two-hop arms, whatever its arity or tokens. Appendix E develops the query language and a context-free grammar schema whose languages are the strategy families, and Appendix E-C extends the grammar to flash loans.

IV. Evaluation

The theorems say what a verdict certifies; this section measures what the system finds. We evaluate the production OCaml module, deployed as the analysis layer of a blockchain forensic platform, against EigenPhi on 220 000 Ethereum blocks and against ArbiNet on a shared 1 000-block subset.

A. Setup and Baselines

We run the system on an arbitrary contiguous range of 220 000 Ethereum mainnet blocks (23 699 751 through 23 919 750, 31 October–1 December 2025), taken within the period for which EigenPhi labels were available; a separate arbitrary 1 000-block range (24 100 000–24 100 999) is used for the three-way comparison. Neither range was selected with any knowledge of what it contained, and every transaction in both is analysed. For each block, we obtain the full execution trace of every transaction via `debug_traceTransaction` on an archive node. The decode layer extracts transfers using the standard ERC token ABIs and WETH, a fixed set shared across all token contracts. The detection algorithm then receives only typed transfer tuples and the call hierarchy; it has no knowledge of Uniswap, Curve, Aave, or any other protocol. Under these conditions the system flags 790 593 transactions, across the four tiers defined below, as exhibiting arbitrage cycle structure. We release the per-transaction verdicts (hash, block, verdict, reasons, cycle count, and per-transaction latency) as a public dataset, enabling independent reproduction of the evaluation without archive-node access.

a) Baselines: No public, independently annotated ground truth exists for per-transaction arbitrage detection; prior work relies on self-collected labels [13], [22] or on third-party MEV data [29]. We therefore compare against the only two systems in this domain whose labels or code we could reuse: *EigenPhi* [30], a production MEV platform that flags 649 790 transactions in the same range, and *ArbiNet* [19], a GNN classifier that, like our analysis layer, needs no protocol-specific ABI catalog. The EigenPhi comparison is deliberately asymmetric, since EigenPhi leverages protocol knowledge our system lacks, so we frame all comparisons as inter-system agreement and analyse the disagreements in both directions.

b) Two vocabularies: Two orthogonal partitions organize what follows. *Tiers* grade our verdicts by the reasons of Algorithm 4: *confirmed* (clean cycles, positive net, no leftovers), *probable* (leftovers remain), *attempted* (cycles whose gas exceeds the profit), and *uncertain* (mixed-sign balances). *Categories* classify agreement with EigenPhi: both flag (Category 1), only we flag, split by tier into confirmed (Category 2) and warning (Category 3); only EigenPhi flags (Category 4). Tiers are properties of one system's output; categories compare two.

Two scope choices inherited from deployment affect the numbers below. Profit is attributed only at the transaction recipient, for the cost-attribution reason of §III-D, so cycles at inner contract addresses are detected but not classified; the disagreement analyses measure what this leaves behind. And the post-fixpoint promotion path scoped by Theorem 3 accounts for 0.8% of detections (6 147). No sampled transaction in §IV-C came from it, so the statistical validation does not cover it. We uniformly sampled 10 promoted detections and inspected their raw traces; all 10 were manually adjudicated

as arbitrages. Otherwise the case rests on the firing conditions, $\tau_{\text{in}} =_{\tau} \tau_{\text{out}}$ with positive delta and no leftovers.

B. Agreement with EigenPhi

The diagnostic reasons partition the 790 593 detections into the four tiers, each with a distinct EigenPhi agreement rate. The *confirmed* tier (469 801 detections, 59.4%) is independently flagged by EigenPhi at 87.2%; *probable* (5.0%) at 70.8%; *attempted* (245 497, 31.1%) at 39.5%, despite the negative net; *uncertain* (4.5%) at 21.0%. This monotonic gradient was not engineered: it emerged from Algorithm 4 and is an independent sanity check, in that the more confident our reasons, the more often the baseline agrees. Overall agreement is 83.5% (542 279 of 649 790; EigenPhi covers profitable and unprofitable cycles), splitting 75.5/5.2/17.9/1.4 across our tiers. The remaining 107 511 EigenPhi-only transactions are analysed in §IV-D.

In the other direction, 248 314 transactions are flagged by our system and not by EigenPhi: 60 199 confirmed (12.8% of all detections), 148 422 attempted, 11 612 probable, and 28 081 uncertain. This volume, invisible to a profit-based detector, is consistent with Li et al. [23] and Chi et al. [22].

C. Manual Validation

We complement the large-scale comparison with transaction-level inspection by the authors: we uniformly sample 100 transactions from each of Categories 1–3 (stratified by tier), resolve addresses via Blockscout, and verify each cycle against the raw trace, the tree reductions, and the economic intent. Every verdict is *structurally verifiable*: the reduced AST, transfer chains, and delta map accompanying each detection constitute an independently checkable certificate, so an auditor can confirm a verdict by inspecting the reduced tree alone, without re-running the reduction (Appendix F demonstrates this on three forensic examples).

a) Category 1: both confirmed (100 txs): All sampled transactions are genuine arbitrages through identifiable DEX pools (7 AMM protocols represented, led by Uniswap V3/V2/V4 and Curve). 91% are single-cycle arbitrages, 9% multi-cycle batches; cycles span 2 to 31 transfer leaves, median 5. 2% involve flash loans. **Zero false positives.**

b) Category 2: ours-only confirmed (100 txs): All 100 sampled exclusive detections are genuine arbitrages. They are larger and more flash-loan-heavy than Category 1: cycle hops median 8 (vs 5), and 51% involve flash loans (vs. 2%), detected without lending-specific logic via leftover recovery's structural pairing. Appendix F-B walks through one such case: a three-hop flash-loan arbitrage that reduces to two closed WETH cycles (17,912 WETH profit, EigenPhi-missed). **Zero false positives.**

Across the 200 confirmed-tier samples of Categories 1 and 2, manual review finds no false positive; a sample of this size bounds the true rate below 1.5% with 95% confidence.[4] All 200 confirmed-tier samples in Categories 1 and 2 came from the fixpoint, so this bound covers the mechanized core and not the 0.8% promotion path.

c) Category 3: ours-only warnings (100 txs): All sampled warning-tier transactions exhibit structurally valid cycles through identifiable DEX pools. Manual review labels 78% attempted arbitrages, 13% uncertain, and 9% probable. 21% are multi-cycle batches (vs 9% in Category 1), 18% involve flash loans, and 38% settle through CoW Protocol (intent-based solver flows whose cyclic structure does not reduce to single-actor arbitrage). The warning tier surfaces these without committing to an arbitrage verdict.

D. Where We Disagree, and Who Adjudicates

Category 4 is the opposite question: what backs the 107 511 transactions EigenPhi flags and we do not? We sample 200 (a larger sample, for tighter forensic statistics), rerun them with full diagnostic output, and inspect the resulting normal forms. All 200 receive a non-arbitrage classification, in three groups. 127 (63.5%) exhibit no arbitrage cycle in normal form: simple transfers, wrap/unwrap operations, RWA-token mints, or yield harvests (Appendix F-C inspects one directly). A further 55 (27.5%) contain structural cycles ($s(C) = d(C)$) whose entry and exit tokens differ: cross-token routing paths, not arbitrages. The remaining 18 (9.0%) contain genuine arbitrage cycles at an inner contract address (flash loan executor, router delegate), not at the transaction recipient: the classification declines to surface them. We adjudicate these 18 as true misses.

This adjudication has a circularity we do not wish to hide: the instrument that classifies the disagreement is our own normal form. The first group is the one a skeptic should press on, and it admits an independent check that never invokes the rewriting: enumerate cycles directly in the decoded transfer graph with a textbook algorithm [31], test closure and token equivalence per Definition 7, and compare the verdicts. We commit to this oracle in the artifact; on the cases already inspected by hand (Appendix F), the trace itself settles the question, since no cycle exists to find.

E. Three-Way Comparison

ArbiNet was trained on blocks 15 540 000–15 585 000 (September 2022); we run the pretrained model unmodified on the 1 000-block range. The three-year gap stress-tests temporal generalization, which a structural detector does not need, though the model's age may disadvantage ArbiNet. Table II reports the eight cells. Of 3 193 transactions flagged by at least one system, all three agree on 1 158; our system covers 81% of ArbiNet's detections and 92% of EigenPhi's. 634 are exclusive to our system: 148 confirmed, 411 attempted, 34 probable, 41 uncertain. For the 432 flagged by a baseline and not classified by us, the gap analysis (rightmost column) repeats the Category-4 methodology: ArbiNet-exclusive detections split into 39.1% inner-address cycles, 45.7% cross-token, and 15.2% with no cyclic structure; EigenPhi-exclusive into 24.7%, 72.7%, and 2.6%.

[4] Clopper-Pearson one-sided upper limit for 0 of 200: 1.49%.

TABLE II

THREE-WAY COMPARISON ON 1 000 BLOCKS. EIG. = EIGENPHI; INNER = ARBITRAGE CYCLE AT AN INNER ADDRESS; X-TOK = CROSS-TOKEN; NC = NO CYCLE IN NORMAL FORM.

	Eig.+	Eig.−	Gap analysis
Ours+ ArbiNet+	1,158	342	—
Ours+ ArbiNet−	627	634	—
Ours− ArbiNet+	74	279	39.1% inner, 45.7% x-tok, 15.2% NC
Ours− ArbiNet−	79	—	24.7% inner, 72.7% x-tok, 2.6% NC

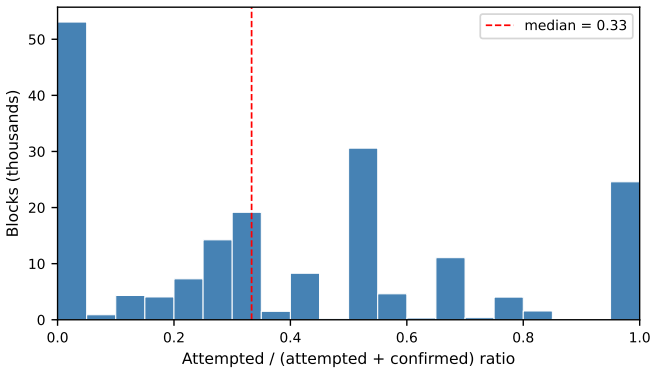

Fig. 4. Per-block attempted / total arbitrage ratio (median = 0.33).

A per-block case study (Appendix H) reveals two qualitative differences. ArbiNet produces false positives on batch settlement protocols (CoW Protocol): the GNN sees cyclic graph topology but does not verify that the tokens match at cycle boundaries (Definition 7). Conversely, ArbiNet misses arbitrages that both our system and EigenPhi confirm, in transactions whose routing contracts postdate its 2022 training data. A structural detector requires no retraining because it operates on transfer events, not on learned representations of specific contracts.

F. Topology, and a Second Query

The reduction finds 940 760 individual cycles across the 790 593 flagged transactions. After structural merging, 89.1% of transactions reduce to a single cycle, 6.7% to two, and 4.1% to three or more (max 82); parallel arbitrages sharing an origin merge into one cycle via R7–R9. Within each cycle, even lengths dominate (an AMM swap produces two transfers), and odd lengths arise from single-token relays. 28.5% of warnings contain leftover cycles recovered by the two-pass procedure of §III-D, and 51% of exclusive confirmed detections involve flash-loan round-trips discovered by its structural pairing. The equivalence queries also run on this data: a second confirmed detection tx_S, built from different tokens through twice the paths, reduces to the same skeleton as tx_R (Appendix E-A).

a) Attempted arbitrages: The *attempted* tier is a further query in the sense of §III-G: the same normal form, asked a different question. Closure and token match are kept, profit positivity is dropped, and what answers is the population of cycles that closed structurally but lost money after gas: 245 497 transactions, roughly half the confirmed count, consistent with a bot that built the same multi-pool cycle as a profitable arbitrage but lost the race, overpaid gas, or encountered unfavourable slippage. Profit-based detectors discard them by construction. At the per-block level, the attempted-to-total ratio clusters at low-denominator fractions (Figure 4): 27.9% of blocks at ratio 0 (only profitable cycles), 16.0% at $1/2$, and 12.9% at 1, blocks whose every cycle lost. The pattern fits small-k competition (a handful of cycles per block) rather than smooth many-bot racing. The ratio-0 mode reflects private orderflow or narrow opportunity windows [29]; the ratio-1 mode is not predicted by the gas-auction model of Daian et al. [32], which assumes a winner, and is consistent with capture via sandwich or off-chain routing [22], [33], [34]. Profit-based detectors see only the winners; structural detection sees both sides.

G. Performance

The system handles arbitrary token counts: observed inputs range from 3 distinct tokens at the median (31.8% triangular) to 106 in the tail. Theorem 2 bounds *passes* at $3n - 2$ and says nothing about the cost of one. As implemented, a pass looks for a partner for each child by walking its remaining siblings, so a pass is quadratic in the worst case and the guaranteed total cubic; in practice every successful rewrite shrinks the child list, and the latencies below stay far from the bound. An index keyed on junction address and token would make the lookup constant-time and the total quadratic; the measurements have not asked for it. The rewriting runs in 0.07 ms median and 0.47 ms P95, under a third of per-transaction cost; the rest is decoding. Including decoding but excluding trace retrieval, the full pipeline completes in 0.25 ms (median), 2.24 ms (P95), and 6.15 ms (P99). 0.02% of transactions containing an arbitrage cycle exceed 100 ms; these are high-transfer transactions (median 181 transfers, max 2008), where the per-pass sibling walk dominates.

V. RELATED WORK

The study of value extraction on Ethereum began with Daian et al. [32], who coined *miner extractable value* (MEV) and documented the priority-gas auctions among arbitrage bots. Qin et al. [29] provided an early systematic measurement ($540M over 32 months), but acknowledged it as a lower bound: only transactions matching known protocol signatures were counted. The SoK of Zhou et al. [35] generalizes this gap beyond arbitrage: across 181 DeFi incidents ($3.24B), cross-protocol composability is the axis existing tools consistently miss.

A first wave of detectors builds aggregate token graphs across blocks. McLaughlin et al. [14] apply Johnson's algorithm to `Transfer` events and uncover 3.8M arbitrages. Zhang et al. [15] search the pool graph itself with a Bellman-Ford variant, finding opportunities rather than executions, and Wang et al. [16] characterize cyclic arbitrages across DEXs.

These methods gain scale but lose the execution context of individual transactions: a forensic analyst cannot reconstruct *how* a profit was realized from an aggregate cycle count. More fundamentally, cycles in the flat transfer graph do not reliably indicate arbitrage: a yield harvest that withdraws and redeposits the same token produces a cyclic flow with matching tokens and positive balance, yet involves no price exploitation (Appendix F-C). Distinguishing such patterns requires the call hierarchy that only per-trace analysis preserves, refining these cycles (Theorem 5).

DeFiRanger [13] and ActLifter [23] identify DeFi actions via protocol-specific event catalogs. DeFiRanger uses a fixed pattern catalog for price manipulation. ActLifter curates 88 events across 10 DeFi actions and clusters bundles to discover new MEV strategies, complementing our per-transaction scope. Chi et al. [22] reduce fragility with exchange-rate checks but still need 44 hand-crafted patterns. None of these provide formal guarantees, and each requires per-protocol catalog extension. Our rewriting system normalizes structurally: one rule covers all protocols sharing a pattern, recovering multi-cycle split-and-merge and lending-based arbitrages without manual extension. Richer trace representations [36], [20], [37] target vulnerability classification, not arbitrage.

Catalog-free machine-learning approaches pursue generality through learned representations rather than algebraic structure. Park et al. [19] propose ArbiNet, a GNN-based classifier that, like our analysis layer, requires no protocol-specific ABI catalog. ArbiNet produces binary labels from training data. Our algorithm reconstructs transfer chains with profit calculations and diagnostic reasons, and offers mechanized formal guarantees. Section IV-E provides a quantitative comparison on 1 000 shared blocks. Jin et al. [17] and Niedermayer et al. [18] classify arbitrage *addresses* and financial bots, answering *who* performs arbitrage but not *how* a given transaction realizes its profit.

Formal-methods approaches split a priori from a posteriori: Clockwork Finance [38] enumerates profitable attacks from protocol specifications, while the Imitation Game [39] replays observed strategies. Our normal forms (Section III-G) partition realized transactions. A formal bridge to Clockwork's symbolic state space is open future work. KEVM [40] formalizes EVM bytecode semantics. We abstract above bytecode, on the typed-transfer view the decoder produces.

MEV strategies compose across transactions [41], [42] and across chains [43], [44]. Cao et al. [45] show that transfer-graph abstractions are structurally incomplete for beneficiary attribution and advocate execution-semantic analysis. Our approach already operates at that level.

Materwala et al. [21] note that existing detectors trade off protocol coverage, per-transaction granularity, and explainability. Ours makes arbitrage one query on a normal-form substrate with mechanized structural soundness and decidable equivalence.

VI. Limitations

a) Trusted base and threat model: We assume an EVM-compatible chain whose traces faithfully reflect consensus semantics: tracing, client consistency, execution visibility and consensus form the trusted base. The theorems apply to the transfers the decoder emits, and an adversary acts on that boundary. The algorithm ignores protocol-specific events, so renaming or omitting them, proxying, or obfuscating control flow gains nothing. *Suppressing* the standard value-movement events, bypassing them through internal balances, or *fabricating* events that move no value: these all split by where the hidden value sits. A transfer missing from a cycle breaks the chain and costs recall, while a hidden cost outside the cycle leaves the structural verdict standing and overstates the reported net. Verdicts are sound about decoded transfers, not about value; cross-checking them against the transaction's state diff would discharge event fidelity, a check we commit to alongside the differential testing of §III-F.

b) Scope: Completeness is not claimed: missing or netted-away transfers silently cost recall, so the recall figures of §IV are measured, not guaranteed. The system reads one transaction's trace and cannot see strategies spanning multiple transactions, bridges, or non-atomic flows, which Heimbach et al. [33] place above 25% of DEX volume; lifting to block level is the natural next step, as a block is a sequence of normal forms and no per-transaction theorem changes. The evaluation covers a single 30-day window; no public historical MEV label sets exist.

VII. Conclusion

The rewriting system is not a detector with formal properties: it is an algebra whose simplest query is detection. Every transaction admits a normal form under the deterministic kernel over its execution-fixed trace order, and the structural equivalence this induces is decidable (Theorem 5), with arbitrage detection as its witness. Cycles emerge from the fixpoint over the call hierarchy and the sender field σ rather than being searched for. The five properties are mechanized in Rocq with no admitted obligation, so the 99.2% of detections that come from the fixpoint are sound over the decoded transfers, and the normal form makes every verdict auditable. On 220 000 blocks it matches a production platform's coverage while surfacing 60 199 exclusive detections and 245 497 attempted arbitrages, a tier profit-based detectors discard.

The same binary runs on Arbitrum and BNB Smart Chain with a configuration change (Appendix G). New annotation predicates should expose liquidations, oracle manipulation, and, with block-level composition, sandwich attacks. Equivalence classes of normal forms partition fund flows into a taxonomy with no manual labeling. The normal forms also suggest an abstract domain for fund flows and a route toward gas-bounded abstract interpretation of smart contracts into that domain.

For now: if it walks like an arbitrage, the normal form confirms it. If it wraps like a sandwich, burns like a liquidation, or . . . , the normal form will carry the answer in its shape.

Ethics Considerations

a) Data: Everything we analyze is public: transactions, execution traces and transfer events recorded on a permissionless blockchain and readable by anyone with an archive node. The system only reads, and every measurement replays history that had already been confirmed, so the experiments cannot have influenced the market they measure. No IRB review was required. That exemption is not the interesting question, though. Addresses belong to people and programs those people wrote, and we publish judgements about what they did, so the risks worth discussing are about the judgements.

b) Dual-use risk: The detection system produces, for each flagged transaction, the complete transfer chains, profit calculation, and pool identifiers. In principle, this output could help a searcher reverse-engineer a competitor's arbitrage strategy. We note three mitigating factors. First, the system operates on *confirmed* transactions: the opportunities it describes have already been executed and are no longer available. Second, the same information is already accessible through commercial platforms (EigenPhi, Flashbots Transparency Dashboard) and on-chain explorers (Etherscan, Blockscout). Our contribution is a *structural representation*, not new data access. Third, operational MEV extraction requires mempool monitoring, gas-price optimization, and sub-second execution infrastructure, none of which the paper provides or discusses.

c) Privacy and de-anonymization: The decode layer enriches addresses with OSINT metadata (contract names, token labels, entity tags) obtained from public sources (Sourcify, 4byte directory, Blockscout). The *analysis layer does not use* these labels: detection operates exclusively on transfer tuples and the call hierarchy (Section II-C). The published dataset contains only transaction hashes, block numbers, structural verdicts, and timing measurements. No OSINT labels, wallet balances, or entity identifiers are included. Transactions appear by hash, as they do on chain; we name no person or organization and do not try to link an address to anyone. Verdicts correlated with address activity could still help de-anonymize a pseudonymous actor, given other data. That is true of any public-chain analysis and not special to us, but it did shape what we release: the dataset is per transaction and aggregates nothing by address, so it describes trades rather than traders.

d) What a verdict means, and what it does not: The system answers one structural question: did value leave an address and come back, in the same asset and in greater quantity. Intent, legality and harm are different questions, and the algorithm has no access to them. The gap matters in both directions. A confirmed arbitrage is often routine market-making that corrects a price difference between pools. And a cycle can close through an address that is not a trading venue at all, in which case the shape is an accident of how the value moved rather than a strategy anyone executed. We saw both while building the evaluation.

Three properties of the design keep that gap from becoming a false accusation. Soundness is claimed for the structural property alone, over the transaction's own transfers (Theorem 3). The tiers abstain: a reconstruction with leftovers or an ambiguous balance returns *Warning* instead of a verdict, which is why only 59.4% of detections are called arbitrages at all. And every verdict carries the reduced tree, the chains and the balances that produced it, so it can be checked rather than believed. A verdict is a place to start looking, not a conclusion about a person, and reading it as the latter, in an enforcement setting and without a human in the loop, is the misuse we would warn against.

e) The legal cases we cite: Section I opens on live proceedings because they show what turns on the question, not because we analyze them. We describe them from public records, analyze no transaction connected to any of them, and take no view on any party. The system has not been validated for evidentiary use and we do not offer it as such.

References

[1] U.S. Department of Justice, "Two brothers arrested for attacking ethereum blockchain and stealing $25m in cryptocurrency," https://www.justice.gov/archives/opa/pr/two-brothers-arrested-attacking-ethereum-blockchain-and-stealing-25m-cryptocurrency, 2024, press release, May 15, 2024. Indictment in *United States v. Peraire-Bueno*, No. 1:24-cr-00293 (S.D.N.Y.); mistrial declared Nov. 2025 after the jury failed to reach a verdict, and a retrial sought by the government for early 2026.

[2] U.S. Commodity Futures Trading Commission, "Cftc charges avraham eisenberg with manipulative and deceptive scheme to misappropriate over $110 million from mango markets," https://www.cftc.gov/PressRoom/PressReleases/8647-23, 2023, press release 8647-23, Jan. 9, 2023. The parallel criminal fraud and manipulation convictions, *United States v. Eisenberg*, No. 1:23-cr-00010 (S.D.N.Y.), were vacated on Rule 29 acquittal in May 2025, the wire-fraud count on the ground that an automated smart contract cannot be the recipient of a false representation; the government's appeal is pending.

[3] European Securities and Markets Authority, "Final report: Guidelines on supervisory practices for competent authorities to prevent and detect market abuse under MiCA," https://www.esma.europa.eu/sites/default/files/2025-04/ESMA75-453128700-1408_Final_Report_MiCA_Guidelines_on_prevention_and_detection_of_market_abuse.pdf, 2025, eSMA75-453128700-1408, Apr. 29, 2025.

[4] H. Adams, N. Zinsmeister, and D. Robinson, "Uniswap v2 core," https://uniswap.org/whitepaper.pdf, 2020.

[5] M. Egorov, "StableSwap – efficient mechanism for stablecoin liquidity," https://curve.fi/files/stableswap-paper.pdf, 2019.

[6] F. Martinelli and N. Mushegian, "Balancer: A non-custodial portfolio manager, liquidity provider, and price sensor," https://docs.balancer.fi/whitepaper.pdf, 2019.

[7] K. Qin, L. Zhou, B. Livshits, and A. Gervais, "Attacking the defi ecosystem with flash loans for fun and profit," in *Proc. Financial Cryptography (FC)*, 2021.

[8] Coinbase, "Around the block – issue 3: The bzx attacks," https://www.coinbase.com/en-fr/learn/market-updates/around-the-block-issue-3, 2020.

[9] palkeo, "The bZx attacks explained," https://www.palkeo.com/en/projets/ethereum/bzx.html, 2020.

[10] Decrypt, "Ethereum DeFi platform MakinaFi hit by flash loan exploit, loses $4m in ETH," https://decrypt.co/355132/ethereum-defi-platform-makina-hit-by-flash-loan-exploit-loses-4m-in-eth, 2026.

[11] EigenPhi, "EigenPhi MEVScan service update," https://eigenphi.substack.com/p/eigenphi-mevscan-service-update, 2026, service notice: free data delivery and public dashboards discontinued Apr. 15, 2026; MEVScan platform shut down June 29, 2026.

[12] ——, "How EigenPhi identifies MEV: Recognizing atomic arbitrage MEV transactions," https://eigenphi-1.gitbook.io/classroom/eigenphis-methodologies/how-eigenphi-identifies-mev, 2023, methodology documentation. Transfers are parsed into a directed transfer graph, strongly connected components are extracted, and a transaction is labeled arbitrage when the token balance nearest the transaction's sender within a component is positive.

[13] S. Wu, Z. Yu, D. Wang, Y. Zhou, L. Wu, H. Wang, and X. Yuan, "Defiranger: Detecting defi price manipulation attacks," *IEEE Transactions on Dependable and Secure Computing*, 2024.
[14] R. McLaughlin, C. Kruegel, and G. Vigna, "A large scale study of the ethereum arbitrage ecosystem," in *Proc. USENIX Security*, 2023.
[15] Y. Zhang, T. Yan, J. Lin, B. Kraner, and C. Tessone, "An improved algorithm to identify more arbitrage opportunities on decentralized exchanges," 2024. [Online]. Available: https://ideas.repec.org/p/arx/papers/2406.16573.html
[16] Y. Wang, Y. Chen, H. Wu, L. Zhou, S. Deng, and R. Wattenhofer, "Cyclic arbitrage in decentralized exchanges," in *Proc. WWW (Companion)*, 2022.
[17] H. Jin, C. Li, J. Xiao, T. Zhang, X. Dai, and B. Li, "Detecting arbitrage on ethereum through feature fusion and positive-unlabeled learning," *IEEE Journal on Selected Areas in Communications*, 2022.
[18] T. Niedermayer, P. Saggese, and B. Haslhofer, "Detecting financial bots on the ethereum blockchain," in *Proc. WWW (Companion)*, 2024.
[19] S. Park, W. Jeong, Y. Lee, B. Son, H. Jang, and J. Lee, "Unraveling the mev enigma: Abi-free detection model using graph neural networks," *Future Gener. Comput. Syst.*, 2024.
[20] K. Qin, Z. Ye, Z. Wang, W. Li, L. Zhou, C. Zhang, D. Song, and A. Gervais, "Enhancing smart contract security analysis with execution property graphs," *Proc. ACM Softw. Eng.*, 2025.
[21] H. Materwala, S. M. Naik, A. Taha, T. A. Abed, and D. Svetinovic, "Maximal extractable value in decentralized finance: Taxonomy, detection, and mitigation," *IEEE Transactions on Services Computing*, 2025.
[22] T. Chi, N. He, X. Hu, and H. Wang, "Remeasuring the arbitrage and sandwich attacks of maximal extractable value in ethereum," 2024. [Online]. Available: https://arxiv.org/abs/2405.17944
[23] Z. Li, J. Li, Z. He, X. Luo, T. Wang, X. Ni, W. Yang, X. Chen, and T. Chen, "Demystifying defi mev activities in flashbots bundle," in *Proc. ACM CCS*, 2023.
[24] F. Vogelsteller and V. Buterin, "EIP-20: Token standard," https://eips.ethereum.org/EIPS/eip-20, 2015.
[25] G. Huet, "Confluent reductions: Abstract properties and applications to term rewriting systems," *J. ACM*, 1980.
[26] R. V. Book and F. Otto, *String-Rewriting Systems*. Springer, 1993.
[27] F. Baader and T. Nipkow, *Term Rewriting and All That*. Cambridge Univ. Press, 1998.
[28] TeReSe, *Term Rewriting Systems*. Cambridge Univ. Press, 2003.
[29] K. Qin, L. Zhou, and A. Gervais, "Quantifying blockchain extractable value: How dark is the forest?" in *Proc. IEEE S&P*, 2022.
[30] "EigenPhi: Real-time MEV analytics platform," https://eigenphi.io, 2024.
[31] D. B. Johnson, "Finding all the elementary circuits of a directed graph," *SIAM Journal on Computing*, vol. 4, no. 1, pp. 77–84, 1975.
[32] P. Daian, S. Goldfeder, T. Kell, Y. Li, X. Zhao, I. Bentov, L. Breidenbach, and A. Juels, "Flash boys 2.0: Frontrunning in decentralized exchanges, miner extractable value, and consensus instability," in *Proc. IEEE S&P*, 2020.
[33] L. Heimbach, V. Pahari, and E. Schertenleib, "Non-atomic arbitrage in decentralized finance," in *Proc. IEEE S&P*, 2024.
[34] A. Capponi, R. Jia, and Y. Wang, "Maximal extractable value and allocative inefficiencies in public blockchains," *Journal of Financial Economics*, vol. 172, 2025.
[35] L. Zhou, X. Xiong, J. Ernstberger, S. Chaliasos, Z. Wang, Y. Wang, K. Qin, R. Wattenhofer, D. Song, and A. Gervais, " SoK: Decentralized Finance (DeFi) Attacks ," in *Proc. IEEE S&P*, May 2023.
[36] M. Zhang, X. Zhang, Y. Zhang, and Z. Lin, "TXSPECTOR: Uncovering attacks in ethereum from transactions," in *Proc. USENIX Security*, 2020.
[37] C. Peng, H. Wang, Y. Wu, H. Wu, M. Fan, Y. Zhao, and T. Liu, "Etrace: Event-driven vulnerability detection in smart contracts via llm-based trace analysis," in *Proc. Internetware*, 2025.
[38] K. Babel, P. Daian, M. Kelkar, and A. Juels, " Clockwork Finance: Automated Analysis of Economic Security in Smart Contracts ," in *Proc. IEEE S&P*, May 2023.
[39] K. Qin, S. Chaliasos, L. Zhou, B. Livshits, D. Song, and A. Gervais, "The blockchain imitation game," in *Proc. USENIX Security*, 2023.
[40] E. Hildenbrandt, M. Saxena, N. Rodrigues, X. Zhu, P. Daian, D. Guth, B. Moore, D. Park, Y. Zhang, A. Stefanescu, and G. Rosu, "Kevm: A complete formal semantics of the ethereum virtual machine," in *Proc. IEEE CSF*, 2018.
[41] B. Guidi and A. Michienzi, "Linking mev attacks to further maximise attackers' gains: evidence from the ethereum blockchain," *Blockchain: Research and Applications*, 2025.
[42] C. F. Torres, R. Camino, and R. State, "Frontrunner jones and the raiders of the dark forest: An empirical study of frontrunning on the ethereum blockchain," in *Proc. USENIX Security*, 2021.
[43] D. Mancino and H. O. Sevim, "Sok: The evolution of maximal extractable value, from miners to cross-chain," 2026. [Online]. Available: https://arxiv.org/abs/2603.07716
[44] C. Ferreira Torres, A. Mamuti, B. Weintraub, C. Nita-Rotaru, and S. Shinde, "Rolling in the shadows: Analyzing the extraction of mev across layer-2 rollups," in *Proc. ACM CCS*, 2024.
[45] Y. Cao, X. Cheng, and Y. Liu, "Peb separation and state migration: Unmasking the new frontiers of defi aml evasion," 03 2026. [Online]. Available: https://arxiv.org/abs/2603.26290
[46] H. Adams, N. Zinsmeister, M. Salem, R. Keefer, and D. Robinson, "Uniswap v3 core," https://uniswap.org/whitepaper-v3.pdf, 2021.

APPENDIX A
GENERATIVE AI USAGE

Anthropic Claude (Opus 4.8, Opus 5, Fable 5) was used as a writing and engineering assistant: to edit and condense author-written text, to check the paper for internal consistency and against the artifact, and, in the Rocq development, for tactic scripts and refactoring under the authors' direction, where every obligation is machine-checked. It also drafted the artifact's documentation files, and raised and drafted much of the Ethics Considerations section, which the authors then revised and adopted as their own. All content, structure, claims, theorem statements, proof strategies, the algorithm and its implementation, the evaluation design, and every experimental number are the authors' own work, and the authors take responsibility for all material in the paper.

APPENDIX B
OPEN SCIENCE

We release the following artifacts, sufficient to evaluate every core contribution of the paper. Item 1 reproduces the formal proofs; items 2–5 reproduce the empirical evaluation.

1) **Rocq formalization.** The file `Arbitrage.v`[5] (5 theorems, 432 lemmas, 13 corollaries, 13 501 lines, no admitted obligation, no added axiom, eleven declared parameters) is self-contained and compiles with `rocq compile Arbitrage.v`. It verifies all five theorems. `rewrite_step` has 17 constructors: the 15 rules R1–R15 of Table I, plus `RS_lift` and the congruence `RS_under`. R16 is modeled by `validated_arbitrage`, which conjoins its gross-delta test with the deployment's cost model `net_positive`, so the mechanized premise bundles R16 with the net-profit gate that §III-E applies afterwards; a cycle passing the first and failing the second is the *attempted* tier (`attempted_arbitrage_characterization`). The step function is computable, making it amenable to Rocq's `Extraction` mechanism. A long-form proof

[5]https://anonymous.4open.science/r/artifact-submission-2128/rocq/Arbitrage.v

companion[6] expands Appendix D and develops the structural-equivalence material of Appendix E at greater length.

2) **Evaluation dataset.** The evaluation rests on three data files. (i) A per-transaction CSV recording the verdict, diagnostic reasons, cycle count, and latency for every flagged transaction across the 220K-block range. (ii) The EigenPhi arbitrage labels for the same range, enabling the cross-reference analysis. (iii) The ArbiNet predictions on the shared 1K-block range, enabling the three-way comparison. Together, these files allow the evaluation pipeline to reproduce every statistic, figure, and table in Section IV without archive-node access.
3) **Evaluation pipeline.** 25 Python scripts orchestrated by `run_all.py` and documented in `METHODOLOGY.md`. Given the evaluation dataset above, the pipeline produces all figures, tables, and summary statistics. The scripts also automate the manual-validation sampling, the Category 4 forensic analysis, and the three-way gap analysis.
4) **Detection tool.** A Docker image containing five compiled binaries (no source code): `inspect_tx_offline` and `batch_analyse_offline` reproduce detection verdicts from pre-exported traces (single-transaction and block-range CSV outputs respectively); `inspect_tx` and `batch_analyse` perform the same two roles against any EVM-compatible RPC endpoint (reviewers can verify any transaction in the paper or test on Arbitrum, BSC, or other EVM chains by changing the RPC URL and wrapped-token address); `export_data` exports raw traces from an RPC node for subsequent offline analysis.
5) **Pre-exported traces.** The full 220K-block evaluation produces over 500 GB of raw execution traces, which exceeds practical artifact hosting limits. We therefore provide raw traces for 1 000 blocks from each evaluation range: the first 1 000 blocks of the main evaluation (23 699 751–23 700 750) and the full 1 000-block ArbiNet comparison range (24 100 000–24 100 999). These traces let the reviewer run the offline binaries, inspect individual transactions, and verify that the detection tool produces the same verdicts recorded in the evaluation CSV. Reproducing the full 220K-block dataset requires an Ethereum archive node with `debug_traceTransaction`; the online binaries and the export binary support this directly.

The detection algorithm is an OCaml module inside a larger open-source blockchain analysis platform and cannot be cleanly factored out of its dependencies (decode layer, OSINT enrichment, database layer) for a self-contained release. In place of a source bundle, reviewers can validate every claim through three independent routes: the Rocq formalization (the algorithm's mechanically verified specification), the compiled binaries (which reproduce every verdict in the paper), and the per-transaction output dataset (which reproduces every figure and table in Section IV).

During review, all artifacts are hosted at https://anonymous.4open.science/r/artifact-submission-2128. Once anonymity is lifted, a link to the public source repository will be added, pinned at the commit matching the submitted version.

APPENDIX C
AMM PRICING AND ARBITRAGE CONDITION

The detector is invariant-agnostic. Across the 220 000-block range, every AMM family we encountered, constant-product (Uniswap v2 [4]), concentrated liquidity (Uniswap v3 [46] and v4), StableSwap (Curve [5]), weighted pools (Balancer [6]), proactive market making (DODO), and adaptive-fee designs (Algebra, Trader Joe's Liquidity Book), exposes the same external interface to the EVM trace: a pair of standard ERC-20 `Transfer` events within a call frame, one for each leg of the swap. Rule R_1 chains the in-leg with the out-leg; rule R_5 handles the Uniswap v4 `PoolManager`, whose singleton design emits `Transfer` events at the manager boundary rather than per pool, so that a pass-through is chained rather than mistaken for a two-cycle. Multi-token pools (Curve n-pools, Balancer 8-token pools) are irrelevant at this layer: the pool's internal n-ary structure collapses to a binary in/out at the trace boundary. The arbitrage condition, different effective exchange rates between two pools holding the same token pair, generalizes uniformly across invariants: it is the existence of a profit-preserving cycle in the realized transfer graph, which our algorithm detects structurally without ever consulting the underlying pricing function.

APPENDIX D
PROOFS

The five theorems of §III-F are mechanized in Rocq ≥ 9.0. The development is one self-contained file of 13 501 lines with no external libraries, comprising the five `Theorem`s, 432 lemmas, 13 corollaries and one worked counterexample, and closing with no `Admitted` obligation and no `Axiom`; `Print Assumptions` on each theorem lists only the eleven declared `Parameter`s described below. The artifact is the authoritative reference.[7] This appendix maps each paper statement to its mechanized counterpart, gives compact proofs whose structure follows the mechanization, and describes the development itself; the artifact also carries a long-form companion that expands these proofs.[8]

A. What Is Guaranteed, and What Is Not

The paper's claims have different standings, and Table III separates them. The distinction that matters most is the last group: the theorems are about the transfers the decoder produces, so decoder fidelity, the correspondence between the production implementation and the mechanized kernel, and any claim about economic intent are outside what is proved.

[6]https://anonymous.4open.science/r/artifact-submission-2128/proofs/proofs.pdf

[7]https://anonymous.4open.science/r/artifact-submission-2128/rocq/Arbitrage.v

[8]https://anonymous.4open.science/r/artifact-submission-2128/proofs/proofs.pdf

TABLE III
STANDING OF EACH CLAIM.

Claim	Standing
No rule invents, drops or duplicates a transfer	mechanized
Reduction terminates under any rule order	mechanized
$3n - 2$ pass bound on fully lifted trees	derived from mechanized budget and step decrease
Balances agree under every rule order	mechanized
Unique normal form under the deterministic kernel	mechanized
Joinable iff equal normal forms; equivalence up to reassociation decidable	mechanized
Verdict yields a Definition 7 witness over T_0's transfers	mechanized; hypotheses hold at T_0
Local joinability up to reassociation	mechanized on well-formed trees
Decoded transfers faithfully reflect value movement	assumed (§VI)
Production module agrees with the extracted kernel	argued, not measured
Promotion path (0.8% of detections)	outside the mechanized core
Economic intent behind a detected cycle	not addressed
Recall	measured, not guaranteed

TABLE IV
PAPER RESULTS AND THEIR MECHANIZED COUNTERPARTS.

Paper	Artifact statement, and what it adds
Thm 1	`theorem_1_preservation`: walk tracking, transfer inclusion, and multiset conservation
Thm 2	`theorem_2_termination`: kernel normal form; the $3n - 2$ bound (`termination_bound`); well-foundedness under every rule order (`rewrite_step_wf`)
Thm 3	`theorem_3_soundness`: verdict *Arbitrage* yields a Definition 7 witness over T_0's own transfers (`def5_witness`)
Thm 4	`theorem_4_confluence`: unique kernel normal form. Clause 2 is `observable_confluence_delta`; clause 3 is `local_confluent_mod_kappa_holds`
Thm 5	`theorem_5_decidable_equivalence`: joinable iff equal normal forms. The coarser equivalence is `struct_equiv_dec`
Def. 7	`def5_witness`: the definition in transfer vocabulary only; its bundle size is pinned by `walk_decomposition_count`
no fabrication	`no_fabricated_transfers`: a chain's transfers are a sub-multiset of T_0's
reported profits	`reported_deltas_are_input_deltas`: every reported balance is a balance of the input trace
plain swap	`plain_swap_not_def5`: a two-leg swap fails Definition 7 on the round-trip clause alone

B. Theorem Map

Table IV pairs each numbered result with the artifact statement that carries it, together with what the mechanization adds beyond the paper's phrasing. The remaining rows are the supporting results the text names.

C. Preservation

A chain C *tracks* walks in G when its transfer sequence decomposes into connected runs, each a walk over edges of E, and the stored endpoints of C are the source of its first transfer and the destination of its last. The invariant holds at T_0, where every leaf is one edge, and is preserved by every rule. Chaining (R1–R6, R10–R12) concatenates two operands whose junction addresses match, so two walks join into one at a shared vertex. Lifting repositions subtrees and touches no chain. Merging (R7–R9, R13) records the union of its operands' walks; the merged chain's transfer list is the concatenation of the operands' lists, so its decomposition into connected runs is the disjoint union of theirs. Annotation (R14, R15) relabels and moves nothing. For conservation, observe that every rule's conclusion carries exactly the transfers of its operands, concatenated: no rule introduces, drops, or duplicates a transfer, so the leaf multiset of any reachable tree is a permutation of T_0's. The mechanization proves the three clauses by one induction over `rewrite_step` and its reflexive-transitive closure. □

D. Termination

Let $u(T)$ count the chains of T not yet labeled and $c(T)$ the total number of children across Tree nodes. Labels are monotonic: annotation only adds them, a merge labels its result at once, and the single downgrade (R16) runs after the fixpoint. The two arguments order the pair differently. The annotation-and-connection loop uses $(u(T), c(T))$. The unrestricted relation uses $(c(T), u(T))$: chaining and merging replace two children by one and lifting removes an internal node, each decreasing c, while annotation holds c fixed and decreases u. Every rule decreases that measure, which gives well-foundedness under every rule order (`rewrite_step_decreases`). For the bound, chains arise only from leaves, so $u(T_0) \leq n$; on a fully lifted, non-empty tree every internal node has at least two children, so by handshaking $c(T_0) \leq 2n - 2$. Each non-trivial pass consumes at least one unit of the budget $u + c$, hence at most $3n - 2$ passes. What is mechanized is the budget $u + c \leq 3n - 2$ (`termination_bound`, composing `unlabeled_le_transfers` with `cc_plus2_le_twice_ct`, the handshake on fully lifted trees) and the loop's progress (`fixpoint_step_det_decreases`); together with the component monotonicity these yield the pass bound. Theorem 2 states the budget, not the derivation length directly. □

E. Soundness

The proof has the three steps announced in §III-F: an inversion, a bridge, and a transfer.

Inversion. The cascade of Algorithm 4 returns *Arbitrage* only when no verdict gate fired, so the reduced tree holds at least one chain C labeled ARB, no leftovers remain, and by hypothesis C survived R_{16}: $\delta_C[s(C), \tau_{\text{in}}(C)] > 0$. The theorem's two structural hypotheses on T_0 need no separate argument: the decoder emits leaves and call nodes only (Definition 2), so T_0 carries no chain, and the requirement that its chains decompose into walks is then vacuous. Both therefore hold of every decoded trace, and the theorem's reach is limited only by the R_{16} premise discussed in §III-F.

Bridge. By preservation, the transfers of C are transfers of T_0, counted with multiplicity (`no_fabricated_transfers`). This is what makes the remaining steps statements about the transaction: every property of C's leaves read off below is a property of edges of G.

Transfer. Four facts about C descend to those edges. First, closure: R14 fires only on $s(C) = d(C)$, and the invariant that a chain's stored endpoints are its first source and last destination makes the underlying edge sequence close at $s(C)$. Second, the token condition: R14 requires $\tau_{\text{in}}(C) =_\tau \tau_{\text{out}}(C)$ on the stored boundary tokens, and the same invariant, for tokens, makes these the tokens of the first and last edge. Third, the bundle: the maximal decomposition of C's edge sequence into connected runs is the witness Definition 7 asks for, and its size is exactly one more than the number of parallel-merge junctions in C (`walk_decomposition_count`), so merge-free cycles yield the classical single closed walk. Fourth, profit: δ_C is the fold of per-transfer balances over C's leaves, so the surviving R_{16} check is the strict positivity of Definition 7's third clause at $v = s(C)$, $\tau = \tau_{\text{in}}(C)$. □

Two supporting facts complete the picture. When no leftovers remain, the cycles partition the non-cost transfers, so the aggregate gross balance is the sum of the per-cycle deltas validated by R_{16}, and the net verdict conditions of Algorithm 4 then bound the aggregate. And when $\tau_{\text{in}} \neq \tau_{\text{out}}$ but the two are $=_\tau$-equivalent, the economically correct check sums the delta over the $=_\tau$-neighborhood of the entry token; this two-element sum is what the post-fixpoint promotion path computes, which is why it lives outside the mechanized core and why Theorem 3 carries its scope hypothesis. The converse of the theorem does not hold, by design: a genuine arbitrage with leftovers or a mixed balance is reported as *Warning*, so soundness excludes false positives and says nothing about false negatives.

F. Uniqueness

Clause 1. Property 1 orders the children of every node by trace position, so the kernel's step is a total function: on any tree it either fires exactly one rewrite, chosen by a fixed scan order, or reports a normal form. A deterministic step admits at most one reduction sequence from any tree; with termination, the normal form exists and is unique.

Clause 2. Every rule permutes the transfer multiset (preservation), and the balance of Definition 3 is a fold over that multiset, so any two trees reachable from T_0, under any rule orders, agree on $\delta[v, \tau]$ at every address and token. This is a conservation argument, not a confluence argument, which is why it holds unconditionally.

Clause 3. Freed from the kernel's order, the relation has genuine critical pairs. Two matter. A bundle of three mutually mergeable chains can associate as $(C_1 \| C_2) \| C_3$ or $C_1 \| (C_2 \| C_3)$: syntactically distinct trees that no further rewriting reconciles. And a chain can be at once an extension operand (R6, R10, R12) and a parallel-merge operand (R7, R13); firing one rule destroys the other's redex. A canonical map resolves the first family: it flattens every nest of merges to its operand list and sorts by trace position, which Property 1 makes a strict order, so both associations have the same image, and the map is idempotent. A tree is *well-formed* when its transfers carry pairwise-distinct trace positions (linearity, true of every decoded tree by construction and preserved by every rule) and no chain that a chaining rule would consume has a parallel-merge twin or a pending annotation in its frame. On such trees, where the second family's overlap is excluded, any two one-step reducts of the same tree rejoin up to this map (`local_confluent_mod_kappa_holds`). Whether the local statement extends to a global one is open; every result in the paper uses the kernel's order and is unaffected. The companion treats the critical pairs of the unrestricted relation, and the exact scope of this theorem and of Theorem 5, at length.[9] □

G. Decidability

If $T \equiv_R T'$, both reduce to a common U, which reduces further to the unique normal forms of each; uniqueness gives $T{\downarrow} = T'{\downarrow}$. Conversely, equal normal forms witness joinability. Computing $T{\downarrow}$ terminates (Theorem 2) and tree equality is decidable, so the word problem is decidable. For the coarser equivalence, the canonical map of clause 3 is computable and idempotent, so comparing images decides equality up to reassociation of parallel merges (`struct_equiv_dec`). □

H. The Mechanized Development

The file reads as one narrative in six parts: the model and the sixteen rules, with R1–R15 as constructors of one inductive relation and R16 as the predicate `validated_arbitrage`; the foundational invariants (the measure, preservation, walk correspondence); the deterministic kernel, a computable step function mirroring the implementation's scan order, with its soundness bridge into the relation; soundness into the transfer graph, where the chain invariants meet `def5_witness`; the five theorems, stated together; and the algebra beyond the paper, where the canonical map, its associativity and commutativity laws, conservation, and the decidable structural equivalence live.

The trust base is eleven `Parameter`s, declared and never defined; no proof assumes anything of them beyond their types. They are the opaque `address` and `token` types with decidable equalities; the token equivalence $=_\tau$; the predicates `is_burn`, `is_mint`, `is_singleton_router` and

[9] https://anonymous.4open.science/r/artifact-submission-2128/proofs/proofs.pdf

`is_token_contract`; the cost model `net_positive`, which makes the theorems parametric in the deployment's gas accounting (the attempted tier of §IV is formally the Definition 7 cycles on which it returns false, `attempted_arbitrage_characterization`); and the trace-order key `trace_key` realizing Property 1's sibling order, which a deployment discharges with the trace's own event indices, unique within a transaction. Two well-formedness conditions are stated and deliberately never assumed, so they are obligations on a deployment rather than hypotheses of any theorem: reflexivity and symmetry of $=_\tau$ (transitivity is not wanted; bridged and pegged assets do not chain), and injectivity of the trace key.

The kernel, the verdict cascade, the canonical map and the decidable equivalence extract to OCaml; the emitted module compiles and runs against placeholder realizers, and the extraction directives (machine integers for the trace key, native lists and options) are erasure-level and carry no logical content. At deployment the parameters are realized by the decoder's concrete types, standard event-signature matching for burn and mint, and the optional router set of R5.

APPENDIX E
STRUCTURAL EQUIVALENCE IN PRACTICE

A. Structural Equivalence by Example

We illustrate structural equivalence on two confirmed arbitrages from the evaluation dataset; the companion develops this material, including the query language and the family grammar, at greater length.[10] The two transactions involve entirely different tokens, different pool contracts, and a different number of internal swaps, yet their reductions converge to the same topological shape.

a) tx_R.: The running example from Section III (Figure 2). A smart contract receives 0.0575 WETH and splits it into three parallel swap paths: one through a WETH/MOON pool, one through CHAD/WETH, and one through DUCK/WETH. Each path converts its intermediate token (MOON, CHAD, DUCK) into BEAN at a dedicated second-hop pool. All three BEAN streams converge on a single BEAN/WETH pool, which returns 0.0598 WETH to the smart contract. The raw trace contains 10 transfer events across 6 pool interactions and produces 16 reduction steps.

b) tx_S.: [11]A different smart contract belongs to the same structural family with more paths. tx_S has the same star topology as tx_R (Figure 2), with six parallel paths through twelve pools instead of three through six: WETH is split across pools PUPPIES, TERMINUS, TOMOE, YFI, CPOOL, and ZETA; each path converts its intermediate token to KABOSU at a dedicated pool, and all six KABOSU streams converge on a single KABOSU/WETH pool. The raw trace contains 19 transfer events across 12 pool interactions.

c) Reduction: Despite their different sizes, both transactions undergo the same reduction sequence. First, leaf chaining (R_1) pairs the inbound and outbound transfers within each pool call frame. After lifting, chain extension (R_6) connects per-pool chains into N multi-hop paths (N=3 for tx_R, N=6 for tx_S). Then, merge (R_7) combines the N paths that share the same origin and destination into a single compound chain, and a final chaining (R_6) appends the return leg. Annotation (R_{14}) recognizes the closed cycle and labels it as an arbitrage.

The normal forms differ only in arity (3 vs. 6 sub-chains) and in the concrete token names. Abstracting over both, $tx_R{\downarrow}$ and $tx_S{\downarrow}$ instantiate the same parametric shape:

$$\text{WETH} \xrightarrow{N \text{ paths}} \tau_i \;\rightarrow\; \text{TARGET} \;\rightarrow\; \text{WETH}$$

Their exact normal forms differ, so comparing normal forms directly separates the two. What they share is the skeleton: applying sk (§III-G) to both and comparing the results decides their common family, and §E-D casts the two tests as queries. Theorem 5 is what makes either comparison decidable. The example is chosen so the shared shape is visually obvious; the same mechanical procedure decides it for transactions whose raw traces hold hundreds of transfers, where visual assessment is impossible.

The equivalence also induces a natural *taxonomy*. At the finest level, two transactions are equivalent iff their normal forms are syntactically identical; tx_R (N=3) and tx_S (N=6) fall in different classes. Quotienting over arity and token identities yields the *parametric families* in which both are one strategy, star-convergent arbitrage with variable N; the next subsection gives the families a finite syntax.

B. A Context-Free Grammar for Strategy Families

Write $\mathsf{Star}(\alpha, L, \alpha)$ for an R14-annotated cycle, $\mathsf{Swap}(\tau, \tau')$ for a single swap, $\circ$ for sequential and $\|$ for parallel composition. For each pair (α, τ') of entry and convergence token, define $G_{\alpha,\tau'} = (\{S, L, C, H\}, \Sigma, P_{\alpha,\tau'}, S)$ with productions

$$\begin{aligned} S &\rightarrow \mathsf{Star}(\alpha,\ L,\ \alpha) \\ L &\rightarrow C \,\|\, L \;\mid\; C \\ C &\rightarrow \mathsf{Swap}(\alpha, \tau_1) \circ H_{\tau_1} \\ H_\tau &\rightarrow \mathsf{Swap}(\tau, \tau') \;\mid\; \mathsf{Swap}(\tau, \tau_k) \circ H_{\tau_k} \end{aligned}$$

Every arm ends at the convergence token τ'; the closing $\tau' \rightarrow \alpha$ swap is the cycle's return, recorded by the Star, not part of any arm. The *star-convergent family* is $\mathcal{L}_{\mathsf{star}} = \bigcup_{(\alpha,\tau')} L(G_{\alpha,\tau'})$.

a) Why context-free: The production $C \rightarrow \mathsf{Swap}(\alpha, \tau_1) \circ H_{\tau_1}$ binds the convergence token τ' across all branches: every arm in a Star must end at the same intermediate token before returning to α. A bottom-up ranked tree automaton does not enforce this, since sibling states are computed independently. Because the nonterminals H_τ are indexed by token, what we give is a grammar *schema*: any finite token vocabulary instantiates it to a finite context-free grammar, in which membership is decidable. In practice Σ is finite and every concrete word is bounded in depth (Theorem 2) and width (the

[10] https://anonymous.4open.science/r/artifact-submission-2128/proofs/proofs.pdf

[11] `0xaa4b2aec9c7a571f96062576135632ece91bde142075963219b26232404dfc5c`

gas limit). New strategy families require only new productions in S, not changes to the rewriting system.

Proposition 1 (Grammar characterization)**.** *Let $T{\downarrow}$ be a normal form containing an arbitrage cycle (Definition 7) with hub address h, entry/exit token α, and one or more parallel swap branches converging at a common intermediate token τ'. Then $T{\downarrow} \in L(G_{\alpha,\tau'})$. Conversely, every word in $L(G_{\alpha,\tau'})$ is the structural image of such a star-convergent arbitrage.*

Sketch. ($\Rightarrow$) By termination and uniqueness (Theorems 2 and 4), the chaining and lifting rules (R1, R6) collapse each branch into a swap sequence $\mathsf{Swap}(\alpha,\tau_1)\circ\cdots\circ\mathsf{Swap}(\tau_{k-1},\tau')$, matching $C \to \mathsf{Swap}(\alpha,\tau_1)\circ H_{\tau_1}$ with H unfolded as needed (finite by termination). Parallel sibling branches at the hub compose via $L \to C \parallel L$. The outer $\mathsf{Star}(\alpha, L, \alpha)$ records that branches return to hub h's account in token α, the closure witnessed by ANNOTATE-CYCLES (R14). ($\Leftarrow$) Any derivation in $G_{\alpha,\tau'}$ exhibits a Star node whose branches route tokens through τ' and return to α; this is a valid CFT normal form by construction, R14 annotates it on structure, and R_{16} confirms $\delta_C[s(C), \tau_{\text{in}}(C)] > 0$ afterwards. □

Both running examples reduce to derivations in $\mathcal{L}_{\mathsf{star}}$, with the same $\mathsf{Star}(\alpha,\ L,\ \alpha)$ skeleton: $tx_R{\downarrow} \in L(G_{\text{weth,bean}})$ with three swap arms and $tx_S{\downarrow} \in L(G_{\text{weth,kabosu}})$ with six. The grammar generates an infinite family; tx_R and tx_S are two concrete members.

C. Extending the Grammar: Flash-Loan Wrappers

Flash-loan-wrapped arbitrages, the family that contains 51% of our exclusive confirmed detections (Category 2, §IV-C), extend the star grammar without changing the rewriting system. The borrow and repay legs of a flash loan form a specular pair (§III-D); leftover recovery removes them from the leaf list and emits a *leftover-cycle* node $\mathsf{LC}(\alpha, a)$ recording the loan token and amount. Leftover cycles are preserved by every later rewrite rule, so they survive into the normal form alongside the star-convergent cycle that uses the borrowed capital.

A normal form is therefore a pair (N, Λ), where N is a star derivation (§E-B) and Λ is a (possibly empty) sequence of $\mathsf{LC}(\alpha,\cdot)$ nodes whose token coincides with the star's hub. Adding the production $\Lambda \to \varepsilon \mid \mathsf{LC}(\alpha, a)\cdot\Lambda$ to $G_{\alpha,\tau'}$ yields the extended grammar $G^F_{\alpha,\tau'}$; when $\Lambda = \varepsilon$ the extension reduces to the star grammar, and the flash-loan family $\mathcal{L}_{\mathsf{flash}} \subset \bigcup L(G^F_{\alpha,\tau'})$ is the subset with Λ non-empty. Membership remains decidable in linear time. Specular pairs on tokens unrelated to the cycle (refunds, meta-transaction relays) do not satisfy any $G^F_{\alpha,\tau'}$ and fall outside the family.

a) The 17 912 WETH arbitrage as a concrete member.: We illustrate on Ethereum transaction `0x45388b0f9ff46ffe98a3124c22ab1db2b1764ecb3b61234e29e5c9732b7fd4ab`, a confirmed arbitrage from the exclusive detections EigenPhi does not flag (full forensic analysis in Appendix F-B). A bot borrows 14 175.71 WETH from an aggregator, executes a three-hop cycle through Bancor, a BNT/AAVE pool, and an AAVE/WETH pool, and repays the loan.

After reduction, the normal form is the pair

$$\begin{aligned} S &= \mathsf{Swap}(\text{WETH}, \text{BNT}) \circ \mathsf{Swap}(\text{BNT}, \text{AAVE}), \\ (N, \Lambda) &= \big(\mathsf{Star}(\text{WETH},\ S,\ \text{WETH}), \\ &\qquad \mathsf{LC}(\text{WETH},\ 14\,175.71)\big). \end{aligned}$$

The single arm ends at the convergence token AAVE, and the closing AAVE → WETH swap is the cycle's return, recorded by the Star exactly as KABOSU → WETH is for tx_S. The word lies in $L(G^F_{\text{WETH,AAVE}})$ and hence in $\mathcal{L}_{\mathsf{flash}}$. The profit unwrap (a separate star on WETH under the native/wrapped equivalence) does not participate in the family-membership test. Membership is decidable in linear time (parse (N, Λ), check leftover-cycle tokens), and well-defined under the deterministic reduction order by Theorem 4.

D. From Detection to Query Language

We write the three queries of §III-G as Q_{arb} (detection), Q_{eq} (exact structural equivalence) and Q_{fam} (family equivalence via the skeleton map sk), add two further queries useful for forensic and monitoring work, and demonstrate Q_{fam} on the running example.

a) Q_{match}: strategy matching.: Given a reference transaction T_{ref}, $Q_{\mathsf{match}}(T) = \top$ iff $T{\downarrow} = T_{\mathsf{ref}}{\downarrow}$. Setting $T_{\mathsf{ref}} = tx_R$ flags every transaction whose normal form exhibits the same three-arm star, regardless of pool or protocol identity.

b) Q_{anom}: structural anomaly.: Given a set S of normal forms previously observed for a bot address, $Q_{\mathsf{anom}}(T) = \top$ iff $T{\downarrow} \notin S$. A bot whose past behaviour is captured by S but later executes a transaction with a different shape (e.g. a four-arm star, a sequential chain) lands outside S and is flagged. Both queries are decidable in polynomial time.

c) Worked example: $Q_{\mathsf{fam}}(tx_R, tx_S) = \top$.: The skeleton map sk erases path length, arity, and token identity (§III-G). On $tx_R{\downarrow} = \mathsf{Star}(\text{WETH}, C_1 \parallel C_2 \parallel C_3, \text{WETH})$, where each C_i is a two-hop chain through BEAN: erasing path length yields $\mathsf{Swap}(\text{WETH}, \text{BEAN})$ per arm; erasing arity collapses the three identical arms to one; erasing tokens gives $\mathsf{Star}(\star, \mathsf{Swap}(\star,\star), \star)$. The same computation on $tx_S{\downarrow}$ (six two-hop arms through KABOSU) yields the same skeleton. Hence $Q_{\mathsf{fam}}(tx_R, tx_S) = \top$ despite different arities, tokens, and pools. A sequential arbitrage (one cycle feeding into the next) would have a different skeleton topology and a different family.

d) Richer queries: Combining structural predicates with the per-cycle balances δ_C (computed during normalization) yields decidable queries such as "arbitrages with profit $> v$ through at least three pools". The number of cycles in $T{\downarrow}$ is finite (Theorem 2), so δ_C-aware queries remain decidable. The rewriting system thus underpins a domain-specific language for fund-flow analysis; this paper instantiates one query, Q_{arb}.

APPENDIX F
FORENSIC CASE STUDIES

The reduced AST is not only a detection artifact; it is a readable record of what happened in a transaction. We demonstrate this on three transactions from the evaluation

dataset: a stablecoin-migration exploit whose profit source only the tree exposes, a confirmed arbitrage that EigenPhi misses, and a complex DeFi operation that *looks* cyclic but is not. In each case the AST tells the full story.

A. A Stablecoin Migration Exploit

Transaction `0x4fe7f35c14e51aa31460c03502928d40c036261234dafba99ef4fa45d0b66904`.

a) Transaction profile: The sender and receiver are the same address (`0xe834...897b`): a self-calling MEV bot. The EVM trace contains 84 internal calls reaching depth 9. The decoded trace yields 14 ERC-20 Transfer events across 5 tokens: agEUR, EURe (Monerium EUR emoney), EUROC, a vault share token, and WETH.

b) AST reduction: The algorithm reduces the initial AST in 10 steps. The final tree contains 10 chain nodes, all with $s(C) = d(C)$ (closed loops rooted at the bot address), plus four leftover leaves. Two of the ten chains satisfy $\tau_{\text{in}} =_{\tau} \tau_{\text{out}}$ and are annotated as arbitrage cycles; the remaining eight are individual swaps:

τ_{in}	τ_{out}	Label	Role
agEUR	agEUR	*arbitrage*	Main cycle
EURe	EURe	*arbitrage*	Profit extraction
agEUR	EURe	chaining	Swap
EURe	EUROC	chaining	Swap
EUROC	agEUR	chaining	Swap
agEUR	WETH	chaining	Residual sale
WETH	ETH	*token burn*	WETH unwrap

The three swap chains reveal the arbitrage route: agEUR enters a pool that returns EURe, the EURe enters a second pool that returns EUROC, and the EUROC enters a third pool that returns agEUR. The fixpoint loop connected these three chains into the main cycle (first row).

c) The token-migration twist: The dominant profit comes from an unexpected source. One of the pools involved in the route holds liquidity in two versions of the same stablecoin: the original EURe contract (`0x3231...273f`) and its post-migration successor (`0x39b8...279d`). When the bot swaps agEUR at this pool, it receives returns denominated in *both* contracts. It routes the new-contract tokens onward through the cycle and keeps the old-contract tokens, netting 2,413 EURe in the process. The algorithm detects this without knowing that a token migration occurred: it simply observes that EURe enters and exits the bot at different amounts, producing a positive delta.

d) Flash loan: The bot funds the operation with a 2,413.95 agEUR flash loan from the Balancer vault. The borrow and repay transfers form a specular pair (same token, same amount, reversed addresses), collapsed into a single leftover cycle $\mathsf{LC}(\text{agEUR}, 2{,}413.95)$ by the recovery pass.

e) Profit: The delta map at the bot address:

	Amount	Token
Gross δ	$+2{,}413.39$	EURe
Gross δ	$+0.000124$	agEUR
Gross δ	$+0.000636$	ETH
Gas cost	-0.000182	ETH
Net	$\mathbf{+2{,}413.39}$	EURe
Net	$+0.000124$	agEUR
Net	$+0.000453$	ETH

f) Verdict: Confirmed arbitrage. Two cycles, zero leftovers, positive final balance. The AST tells the full story: the arbitrage route, the funding mechanism (Balancer flash loan), and the profit source (old vs. new EURe contract) are all readable from the reduced tree, without any knowledge of the contracts involved.

B. A 17,912 WETH Arbitrage That EigenPhi Misses

This is the flash-loan arbitrage introduced in §E-C (tx `0x45388b0f9ff46ffe98a3124c22ab1db2b1764ecb3b61234e29e5c9732b7fd4ab`). Three anchors: 17,912 WETH gross cycle profit (17.72 in, 17,930 out), 14,175.71 WETH flash-loan borrow/repay, 13,088 ETH builder bribe. EigenPhi misses it; our system confirms. Here we summarise the reduced AST and the profit accounting.

a) Transaction profile: The EOA (`0x5884...7d47`) calls a bot contract (`0x06cf...f5ef`). The trace is compact: 42 internal calls reaching depth 8, with only 6 ERC-20 Transfer events across 4 tokens: WETH, BNT (Bancor Network Token), AAVE, and native ETH.

b) AST reduction: The algorithm reduces the AST to two chains both labelled *arbitrage* and both WETH $\to$ WETH closed on the bot address with zero leftovers: a main cycle and a profit unwrap. The seven legs of the main cycle, in order, are: the bot wraps 17.72 WETH at the WETH contract, sends the resulting 17.72 ETH to Bancor and receives 122,365 BNT, forwards the BNT to a BNT/AAVE pool which returns 128.6 AAVE, and the AAVE/WETH pool returns 17,930 WETH to the bot.

c) The price discrepancy: The AST reveals a striking imbalance: 17.72 ETH buys 122,365 BNT at Bancor, which buys 128.6 AAVE, which is worth 17,930 WETH at the AAVE/WETH pool. This is a $1{,}000\times$ return through a three-hop path. The discrepancy is at the AAVE/WETH pool, which overvalues AAVE relative to Bancor. Whether this reflects a temporary liquidity event, a governance action, or a pool manipulation is beyond the scope of the algorithm; the AST records the flows and the profit, leaving the interpretation to the analyst.

d) Flash loan and builder payment: The bot borrows 14,175.71 WETH from an aggregator (`0xbbbb...ffcb`); the borrow/repay pair reduces to a single leftover cycle $\mathsf{LC}(\text{WETH}, 14{,}175.71)$. The bot unwraps the remaining WETH and forwards 73% of the gross profit to the block builder as a priority-inclusion bribe.

e) Verdict: Confirmed arbitrage: two cycles, zero leftovers, gross $+17{,}912$ WETH netting to $+4{,}824$ ETH to the EOA after the 13,088 ETH builder bribe and gas. The entire

analysis derives from 6 ERC-20 transfers and 8 ETH value transfers, with no knowledge of Bancor, AAVE, or any of the pool contracts involved.

C. A Yield Harvest That Looks Like an Arbitrage

Transaction `0x5d44c672cce36070dae0419d4cd2852f05bac823637e2eb58e2c403847c080d9`.

EigenPhi flags this transaction as an arbitrage. Our system does not. The disagreement does not rest on the rewriting: the decoded transfers alone show that no token returns to its origin in the denomination it left in, and that the sender's net balance is negative. Either fact can be checked against the trace without running the reduction. The reduced AST is how we present that conclusion compactly, not how we establish it.

a) Transaction profile: The EVM trace is large: 346 internal calls reaching depth 11, with 24 ERC-20 Transfer events across 11 distinct tokens. The tokens include WETH, USDC, CRV, CVX, crvUSD, frxUSD, and five LP or vault share tokens. At first glance, the transaction resembles a complex multi-venue arbitrage.

b) AST reduction: The algorithm constructs the initial AST (31 leaf nodes) and reduces it in 13 steps. The final tree contains 8 chain nodes, all with closed loops ($s(C) = d(C)$), plus leftover transfers and burns.

c) Closed-loop analysis: The reduction yields eight closed loops, but *none* has $\tau_{\text{in}} =_\tau \tau_{\text{out}}$: three are LP unwraps from a single Curve LP contract (entry token `ecb0`, exits to `c0c17dd0`, `crvUSD`, and a CVX→WETH reward sale); three are stable swaps among `crvUSD`, `frxUSD`, `c0c17dd0`, and USDC; and the remaining two are a USDC→WETH swap and a CRV reward sale through the WETH/CRV pool.
Every row is a swap: tokens enter and exit the same address, but in different denominations, so no row satisfies R14 or R15. USDC, which both enters and exits the central contract, converges from multiple pools to the sender rather than returning to its origin: the pattern is a funnel, not a cycle.

The overall token flow is linear: LP tokens → ecb0 → c0c17dd0/crvUSD → frxUSD → crvUSD → USDC → EOA, with side branches for CRV and CVX reward claims sold for WETH and then for USDC. This is a *yield harvesting* operation: the sender burns LP tokens from a Curve vault, claims accrued rewards, converts everything to USDC, and withdraws. No token completes a round trip, and the final balance is negative (gas exceeds the tiny ETH residual), consistent with a position unwind rather than a profit-seeking trade. Not an arbitrage: no chain the reduction builds returns in the asset it left in, and the final balance is negative. The algorithm reaches this conclusion without knowing what Curve, Convex, or any of the vault contracts are: 24 transfers, 8 closed loops, no matching boundary tokens. For completeness we also ran ArbiNet [19], the GNN baseline of Section IV, on this transaction's block: it does not flag the transaction, so the false positive is specific to EigenPhi here, not to flow-based detection as a class.

d) What a flat detector sees, and why: Projected onto the transfer graph (Definition 1), this transaction does contain address-level cycles: three tokens both enter and leave the central contract. On this graph, EigenPhi's documented pipeline [12] fires mechanically: every pool swap sends one token out and receives another back, so the contract and its pools are mutually reachable and collapse into one strongly connected component, and the sender's 19,212 USDC satisfies the positivity test. Yet the component is not a traversable trading route: no sequence of transfers carries value round, because the token handed on at each junction is not the token received. What the aggregate view shows is only that the same asset came in and went out, in these amounts:

round trip	out	in	balance
WETH	0.0492	0.0492	0
LP token	23,048.44	23,048.44	0
crvUSD	30,719.00	30,716.40	−2.60

The WETH row is the one that most resembles an arbitrage. It is real in the aggregate: 0.0492 WETH leaves the contract for a WETH/USDC pool, and 0.0488 and 0.0004 WETH come back from the pools where the position's CRV and CVX rewards were sold. The sum is exact, so the contract gains nothing.

Neither does any of it compose into a chain. The outgoing transfer and the two returning ones were emitted by three different calls, at depths 9, 8 and 7 of the call tree, so they are never siblings and no chaining rule can join them. Even setting the call structure aside, the tokens do not line up: the contract receives USDC from the pool it sent WETH to, and what it sends next is CRV, so there is no continuity to chain on. The reduction therefore does not build a cycle here and reject it on its balance; it builds no such cycle at all. The sender settles the question on its own: it holds a single edge in the whole graph, receiving 19,212 USDC and sending nothing, so it lies on no cycle.

APPENDIX G
CROSS-CHAIN PORTABILITY

The rewriting system depends only on the deterministic sequential execution property shared by all EVM-compatible chains (Property 1), not on Ethereum-specific assumptions. As a portability smoke-test of the model (not a cross-chain evaluation), we ran the detection algorithm on two chains it was never designed or tested against: Arbitrum One (an Ethereum Layer-2 rollup) and BNB Smart Chain (an independent EVM-compatible Layer-1).

A. Arbitrum

a) Setup.: We selected 1 000 consecutive Arbitrum blocks (447 413 490–447 414 489) containing 23 250 transactions. The detection binary was compiled from the same source code used in the main evaluation (§IV), with a single configuration change: the wrapped-asset address was set to the Arbitrum WETH contract (`0x82aF49447D8a`) via an environment variable. No rewriting rule, no threshold, and no annotation predicate was modified. The algorithm received raw

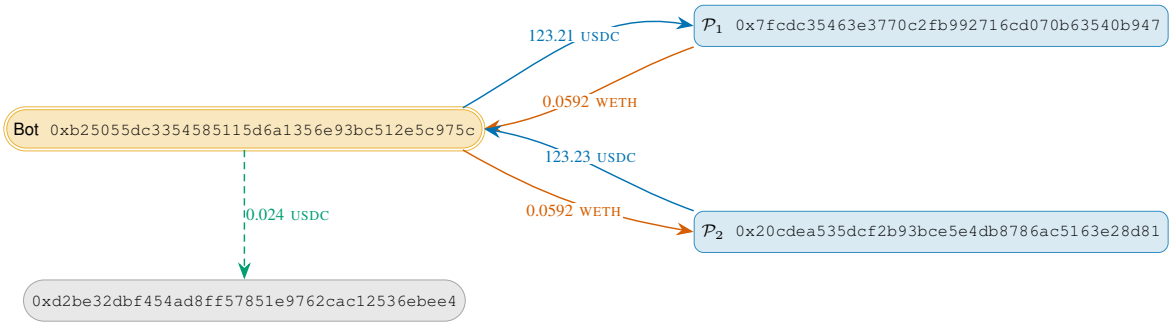

Fig. 5. Transfer graph of an Arbitrum arbitrage (tx `0x1472c663`). Blue: USDC (`0xaf88d065e77c`); vermillion: WETH (`0x82aF4944`); dashed: surplus forwarded to an external address. Detected with no code changes; only the WETH address was configured.

transaction traces from an Arbitrum RPC node and processed them through the same decode–analyse pipeline used for Ethereum mainnet.

b) Results.: Of the 23 250 transactions, the system classified 50 as confirmed arbitrages and 952 as warnings (4.3% flagged overall). Confirmed arbitrages average 2.0 cycles per transaction. The lower detection rate compared to Ethereum mainnet reflects Arbitrum's different transaction mix: most L2 activity consists of user-initiated swaps and transfers rather than MEV bot strategies.

c) Case study.: We examine one representative transaction in detail.[12] The bot contract (`0xb250`) sends 123.21 USDC to pool $\mathcal{P}_1$ (`0x7fcd`), which returns 0.0592 WETH. The bot forwards the entire WETH amount to pool $\mathcal{P}_2$ (`0x20cd`), which returns 123.23 USDC (Figure 5). The USDC surplus (0.024 USDC) is forwarded to a separate address, which may be a profit receiver, a vault, or part of a larger multi-transaction strategy. The system classifies this transaction as *Warning* rather than *Arbitrage* because the bot's final balance is mixed: it is net positive in USDC but net negative in ETH (consumed as gas). Without a price oracle, the algorithm cannot determine whether the overall position is profitable, so it conservatively issues a warning.

d) Structural equivalence.: After rewriting, the reduced form of this Arbitrum transaction is structurally identical to the triangular arbitrages in the Ethereum evaluation: a single annotated cycle with two chained swaps and a leftover extraction. The same rules fired in the same order and produced the same canonical shape, despite differences in gas pricing, block timing, and pool contract implementations between the two chains.

B. BNB Smart Chain

a) Setup.: To test portability to an independent Layer-1, we ran the same binary on 1 000 consecutive BNB Smart Chain (BSC) blocks (91 308 000–91 308 999). The only configuration change was the wrapped-asset address, set to the BSC WBNB contract (`0xbb4CdB9Cbd36`) via the same environment variable. BSC carries 3-second block times and a mix of legacy (type 0x0) and EIP-1559 (type 0x2) transactions in the same block; the decode layer handles EIP-1559 natively and treats legacy transactions as outside its current scope. Legacy transactions are not malformed: they simply use a pre-1559 fee field layout the decoder does not unpack. Extending coverage would be a decoder patch, not an algorithmic change; we keep them out of the sample so the figures below are reported against a single transaction shape.

b) Results.: The 1 000 blocks contain approximately 105 000 transactions. Of these, 38 126 are EIP-1559 (36%) and the remaining 66 874 are legacy (64%). The detection rate is reported against the EIP-1559 denominator: 88 confirmed arbitrages and 922 warnings out of 38 126 EIP-1559 transactions (2.6% flagged overall). Against the full 105 000 the rate is mechanically lower (0.96%), but that figure conflates a covered sub-population with an out-of-scope one and is not a meaningful comparison with the Ethereum and Arbitrum baselines, which run on the post-merge single-format era. Confirmed arbitrages average 1.2 cycles per transaction, with a maximum of 3. Warnings split into attempted arbitrages (negative profit after gas, 68%) and real cycles downgraded by leftover transfers (32%), matching the distribution observed on Ethereum and Arbitrum.

c) Case study.: We examine one confirmed arbitrage in detail.[13] The bot contract (`0xaf70`) sends WBNB to pool $\mathcal{P}_1$ (`0xe3c1`), which returns token `0xf310`. The bot forwards it to pool $\mathcal{P}_2$ (`0x3cd4`), which returns token `0x570a`. Finally, pool $\mathcal{P}_3$ (`0xbffe`) converts back to WBNB with a positive surplus. The fixpoint labels the composed cycle as an arbitrage (R14) with a positive WBNB balance and zero leftovers: a clean confirmed arbitrage.

d) Structural equivalence.: After rewriting, the reduced form of this BSC transaction is structurally identical to the triangular arbitrages on Ethereum and Arbitrum: a single annotated cycle with three chained swaps, each through a different pool. The same rules (R1 for leaf chaining, R14 for annotation) fire in the same order and produce the same canon-

[12] `0x1472c66337ca2caca95b7e5c619cd85c4caa5c7d29292b2dc8966b8bd3ed6d42`

[13] `0x83c2295b1c17312a0598bb6dc6b9f8f12646f48b30a0423397c8acd7e2504d26`

ical shape, despite differences in block times, gas pricing, and pool contract implementations across the three chains.

C. Implications

The two case studies confirm three properties of the approach. First, the rewriting rules, the sender enrichment σ, and the cycle-annotation logic transfer without modification to chains with different consensus mechanisms (Arbitrum's centralized sequencer vs. BSC's Proof of Staked Authority), block times (sub-second vs. 3 s), and gas pricing models. The only chain-specific parameter is the wrapped-asset address, a deployment constant. Second, OSINT labels (pool names, protocol tags) are unavailable on both Arbitrum and BSC, yet detection operates correctly without them. This confirms the architectural separation between the decode and analysis layers: the algorithm reasons over token flows and sender fields, not over external metadata. Third, the detected arbitrages on all three chains exhibit the same structural patterns (triangular, multi-hop, batched), produced by the same fixpoint rules. MEV strategies are chain-agnostic in structure; only the token addresses and pool contracts differ.

a) Beyond the EVM.: The three validations cover EVM-compatible chains, where the trace format is identical by construction. Property 1 also holds for non-EVM virtual machines. Porting to Solana's SVM, for instance, would require only a new decode layer: SPL Token instructions (not events) provide the transfer tuples, and Cross-Program Invocations form a call tree analogous to nested `CALL` frames. The σ field maps to the CPI invoker. The rewriting rules, the fixpoint, and all formal properties would remain unchanged.

Appendix H
ArbiNet Comparison: Case Study

To understand the qualitative differences between the structural and GNN-based approaches, we examine a randomly chosen block 24 100 069 in detail.[14] Of its 311 transactions, ArbiNet flags 5 as arbitrages and our system flags 5 as arbitrage and 1 as warning (Table V). The results are manually checked.

a) Three-way agreement.: Transactions `0x4573`, `0xf170`, and `0x0fdc` are flagged as arbitrage by all three systems. These form a high-confidence consensus set: three independent approaches (protocol-specific heuristics, GNN classification, and structural rewriting) agree on the same transactions.

b) Partial agreement.: Transaction `0x12f4` is classified as *arbitrage* by ArbiNet and as *warning* by our system; EigenPhi does not flag it. The cyclic structure exists and the cycle is correctly identified, but gas costs exceed the gross profit, producing a mixed final balance. This is a correct verdict under the graduated confidence model (§III-E): the cycle is real, but the final balance is mixed (positive in one token, negative in another after gas), making the economic outcome indeterminate without a price oracle. EigenPhi's absence is consistent: the transaction's profitability is unclear, and EigenPhi may require a definitive positive balance.

[14]Full transaction hashes are recoverable from any Ethereum explorer by matching the short prefix within the block.

TABLE V
Per-transaction verdicts. A = ArbiNet, O = Ours, E = EigenPhi. TP = true positive (confirmed arbitrage); FP_A/FN_A = ArbiNet false positive/negative. Assessment based on manual AST inspection.

Tx	A	O	E	Assessment
`0x4573`	arb	arb	arb	TP, 3/3 agree
`0x12f4`	arb	warn	—	TP, mixed final balance
`0xf170`	arb	arb	arb	TP, 3/3 agree
`0x8dc9`	arb	—	—	FP_A: CoW, $\tau_{in} \neq \tau_{out}$
`0x0fdc`	arb	arb	arb	TP, 3/3 agree
`0x4744`	—	arb	arb	FN_A: 3-pool, post-2022
`0x9d71`	—	arb	arb	FN_A: V4, post-2022

TABLE VI
`0x8dc9`: ArbiNet false positive. CoW Protocol batch settlement: both cycles have $\tau_{in} \neq \tau_{out}$ (USDC $\neq$ USDT).

	From → To	Amount	Token
Cycle 1 (cycle, not promoted)			
1	`0xe6eb...e6eb` → CoW Settlement	1 022.06	USDC
2	CoW Settlement → `0xe6eb...e6eb`	1 022.47	USDT
Cycle 2 (composite, not promoted)			
swap 1: USDC → BOLD *(Balancer)*			
1	CoW Settlement → Balancer vault	1 021.88	USDC
2	Balancer vault → CoW Settlement	1 022.84	BOLD
swap 2: BOLD → USDT *(Uniswap V4)*			
3	CoW Settlement → Uniswap V4	1 022.84	BOLD
4	Uniswap V4 → CoW Settlement	1 022.50	USDT

We now turn to the cases where the systems disagree fundamentally.

c) ArbiNet false positive (`0x8dc9`).: This transaction is a CoW Protocol batch settlement routing through Balancer and Uniswap V4. ArbiNet classifies it as an arbitrage; our system disagrees. Table VI shows the reduced AST: two closed-loop chains, both labeled *cycle*. In Cycle 1, a user sends USDC and receives USDT; in Cycle 2, the settlement routes USDC through an intermediate token (BOLD) and returns USDT. Both cycles have τ_{in} = USDC $\neq$ τ_{out} = USDT: the token equivalence $=_\tau$ identifies only the native/wrapped pair (ETH/WETH), not stablecoins. Our system correctly reports zero arbitrage cycles. One possible explanation is that ArbiNet's GNN treats stablecoins as interchangeable: both are pegged to \$1, so a USDC→USDT flow looks economically equivalent to a same-token cycle. But structurally it is not: the arbitrage condition (Definition 7) requires token-equivalent boundaries, not price equivalence.

d) ArbiNet false negative: `0x4744` (multi-hop, 3 pools).: Both our system and EigenPhi confirm this as an arbitrage; ArbiNet misses it. Table VII shows the reduced AST: the bot routes WETH through Balancer (→ MKR), Bancor (→ BNT), and a third pool (→ ETH). The fixpoint labels the composed

TABLE VII

0x4744: ARBINET FALSE NEGATIVE. 3-POOL MULTI-HOP ARBITRAGE: τ_{in} = WETH $=_\tau$ τ_{out} = ETH. PROFIT: $+2.0 \times 10^{-5}$ WETH.

	From → To	Amount	Token
Cycle 0 (arbitrage, fixpoint)			
swap 1: WETH → MKR *(Balancer)*			
1	Bot → Balancer	0.0105	WETH
2	Balancer → Bot	0.0205	MKR
swap 2: MKR → BNT *(Bancor)*			
3	Bot → Bancor	0.0205	MKR
4	Bancor → Bot	77.47	BNT
swap 3: BNT → ETH *($Pool_3$)*			
5	Bot → $Pool_3$	77.47	BNT
6	$Pool_3$ → Bot	0.0105	ETH
Cycle 1 (token mint, not promoted)			
1	Bot → WETH	0.01049	ETH
2	WETH → Bot	0.01049	WETH

TABLE VIII

0x9D71: ARBINET FALSE NEGATIVE. V4 TRIANGULAR ARBITRAGE: τ_{in} = ETH $=_\tau$ τ_{out} = WETH. PROFIT: $+7.2 \times 10^{-6}$ WETH.

	From → To	Amount	Token
Cycle 0 (arbitrage, fixpoint)			
swap 1: ETH → *0xaf04 (V4)*			
1	Bot → V4	0.00666	ETH
2	V4 → Pool	596.56	0xaf04
swap 2: 0xaf04 → WETH *(Pool)*			
3	Pool → Bot	0.00666	WETH
Cycle 1 (token burn, not promoted)			
1	Bot → WETH	0.00666	WETH
2	WETH → Bot	0.00666	ETH

cycle as arbitrage: τ_{in} = WETH $=_\tau$ τ_{out} = ETH, $s(C) = d(C)$ = Bot. A second cycle (token mint) wraps the profit from ETH to WETH. ArbiNet misses this transaction because the routing contracts are absent from its 2022 training data.

e) ArbiNet false negative: 0x9d71 (Uniswap V4, triangular).: The pattern repeats with a different topology. Table VIII shows the reduced AST: the bot sends ETH through the Uniswap V4 singleton router (→ 0xaf04), then a second pool converts back to WETH. The fixpoint labels the cycle as arbitrage: τ_{in} = ETH $=_\tau$ τ_{out} = WETH. A second cycle (token burn) unwraps the settlement. Again, ArbiNet misses it because the V4 singleton postdates its training data.

f) Emergent swap identification.: ERC-20 mandates `Transfer` events but not swap-specific events such as `Swap` or `TokenExchange`. Any pair of `Transfer` events with complementary directions and the same σ is structurally a swap, regardless of declared events. For a Curve/Uniswap-V3 transaction the algorithm recovers 10 swaps from transfers alone, where the contracts emit only 4 `Swap` events, revealing pool interactions invisible to event-based decoding. Swap structure is not an input to the algorithm; it is an output.

g) Summary.: The case study illustrates three structural advantages of the rewriting approach over GNN-based classification. First, the token-identity condition at cycle boundaries filters false positives that graph-topology classifiers cannot distinguish. Second, the fixpoint produces formally guaranteed detections on contracts absent from any training set, eliminating temporal degradation. Third, the reduced AST is a readable decomposition of fund flow into constituent swaps, providing the analyst with an explainable structural account.